Day-to-day dynamics with advanced traveler information

Hongbo Ye [a], Feng Xiao [b,*], and Hai Yang [c]

[a] *Department of Civil Engineering and Industrial Design, University of Liverpool, United Kingdom*

[b] *School of Business Administration, Southwestern University of Finance and Economics, PR China*

[c] *Department of Civil and Environmental Engineering, The Hong Kong University of Science and Technology, Clear Water Bay, Kowloon, Hong Kong, PR China*

Abstract

This paper studies how the advanced traveler information affects the stability of the day-to-day flow evolution of a transportation system. Two scenarios are investigated regarding the types of information provided, where one type is the historical travel time and the other the forecasted travel time. Given the information, travelers are assumed to form their own perception/prediction on travel time and further choose the routes. The day-to-day dynamics under the two above-mentioned scenarios are formulated using both discrete-time and continuous-time models, and their respective local stability is analyzed. Findings from the discrete-time and continuous-time models are compared, which show that: (i) the discrete-time models behave in a more complex fashion than the continuous-time models, and (ii) the conclusions drawn from the discrete-time modeling and continuous-time modeling can be consistent, different or contradictory, which depends on the system parameters, network structure, the travel time functions and the route choice probability functions.

Keywords: day-to-day dynamics; advanced traveler information; traveler learning and prediction; travel time forecast

* Corresponding author. Email: xiaofeng@swufe.edu.cn

1. Introduction

In the transportation networks, travelers make trip decisions based on their experience and knowledge about the network. With the development of information and data technologies, nowadays, the traffic conditions can be collected and processed almost in real time. Such information can be accessed by the potential trip makers in a fast and comprehensive manner, in the form of Advanced Traveler Information (ATI), via e.g. their smart devices. The ATI can include historical, real-time and predicted/forecasted travel information, and can easily influence travelers' day-to-day travel decisions including modes, routes, and departure time. Studying how these travel decisions are affected by ATI would help justify the benefits of ATI, and help predict the daily travel demand. The latter is important for the day-to-day traffic management and control, such as road tolls (Guo, 2013; Guo et al., 2016; Ye et al., 2015) and signal settings (Smith and Mounce, 2011; Xiao and Lo, 2015). Among the various travel decisions, this paper focuses on route choice.

With the implementation of ATI systems (ATISs), travelers' route choice will be increasingly dependent on the ATI, which means the ATI provided will have a great impact on the evolution of the traffic demands and flows from day to day. Such impact has been widely researched but mainly via simulation (Emmerink et al., 1995; Hu and Mahmassani, 1997; Jha et al., 1998; Liu et al., 2017) and human-participating lab experiments (Mahmassani and Stephan, 1988; Qi et al., 2019; Rapoport et al., 2014; Yang et al., 1993). Less attention has been paid to the mathematical/analytical properties (in particular, the stability) of the evolution process, and most of these mathematical/analytical analyses were focused on the historical and real-time information, where the most common assumption is that the travelers know the actual travel time of the previous day(s) (Horowitz, 1984; Cantarella and Cascetta, 1995; Huang et al., 2008). However, besides providing historical records, the transportation agencies can actually manage and control the network in a more proactive manner by, e.g., forecasting the travel time in the coming day (Cho and Hwang, 2005; Friesz et al., 1994) and feeding the travelers with the forecasted information rather than the historical one. A natural question is then, how such strategical change on the information provision would influence the behavior and properties of the transportation system regarding the evolution of traffic flows from day to day, and whether the system would benefit from it. Such question is rarely theoretically discussed in the literature. Bifulco et al. (2016) assumed the coexistence of

equipped and non-equipped travelers and rigorously proved the stability of the system under perfect information (i.e., the forecasted travel time is exactly the same as the travel time that the travelers will experience); numerical studies were also conducted to examine the impact of imperfect information and ATIS market penetration rate on the network stability, while the theoretical analysis was not provided. Similarly, Delle Site (2018) also assumed the perfect information and considered an additional type of users who have the knowledge of free-flow travel time in the network; however, the stability of the proposed model was not analyzed. In a word, both Bifulco et al. (2016) and Delle Site (2018) assumed that the ATIS can accurately estimate the travel time that the travelers will experience, which is difficult to be satisfied in reality. A more realistic assumption was considered in Liu et al. (2017) for investigating the day-to-day departure time choice, which assumed the ATIS to update its forecast using the linear filtering; however, a general stability condition was not provided. Adopting the idea of Liu et al. (2017) for route choice, Li et al. (2018) further assumed that ATIS's forecast can have a certain level of inaccuracy (i.e., the forecasted travel time are proportional to the travel time that the travelers will experience) and rigorously proved the stability of their day-to-day dynamical system. However, the proportionality assumed by Li et al. (2018) is still a strong assumption which is dependent on the forecasting algorithms used by the ATIS and is not necessarily satisfied in practice. Therefore, in this paper, instead of assuming the accuracy of the forecast, we explicitly model ATIS's travel time forecasting rule and discuss how it can influence the stability of the day-to-day flow evolution.

The day-to-day flow evolution can be studied by setting up appropriate day-to-day models. In this paper, we use the deterministic-process day-to-day models, which are formulated as ordinary differential equations or difference equations with a set of equilibrium points as steady states[1]. There are two major ways in constructing a deterministic-process day-to-day model. On one hand, one can assume that the travel demands are inclined to switch from slower routes to faster routes and that the flow adjustment rate is determined by the revealed flows and actual travel time. The resultant models include the "rational behavior adjustment process" (RBAP) (Guo et al., 2013, 2015; Yang and Zhang, 2009; Zhang et al., 2001), those embraced by the RBAP framework (Friesz et al., 1994; Han and Du, 2012; He et al., 2010;

[1] There's another important type of day-to-day model which formulates the flow change as a stochastic process, or more specifically a Markov chain/process, whose steady state is the equilibrium probability distribution. The research can be traced back to Cascetta (1989) and was reviewed recently by Watling and Cantarella (2015).

Jin, 2007; Nagurney and Zhang, 1997; Smith, 1984; Smith and Mounce, 2011) and others (e.g., Smith and Watling, 2016; Xiao et al., 2016, 2019; Ye and Yang, 2017). On the other hand, one can treat the change of network flows as a result of the change of travelers' perception or prediction on the future travel time. Such idea was adopted in Bie and Lo (2010), Cantarella and Cascetta (1995), Horowitz (1984), Watling (1999), Xiao and Lo (2015), Xiao et al. (2016) and Ye and Yang (2013), just to name a few, and will also be used in this paper.

When formulating a day-to-day model, the "day" can be assumed either continuous or discrete, where both were widely used in the literature. The discrete-time models are a more realistic representation of the real world, while the continuous-time models are more convenient for mathematical and analytical analysis on the stability. Meanwhile, the stability properties of a continuous-time model can indicate the stability of its discrete-time counterpart (Watling, 1999). Therefore, in this paper, we start with the discrete-time models but also derive and study their continuous-time counterparts. The theoretical analyses and case studies on these models enable us to investigate and compare the stability[2] of the day-to-day evolution processes without or with the travel time forecast of ATIS. It is found that, the discrete-time models behave more complicatedly than the continuous-time models, and the two modeling techniques can give consistent, different or even contrary results.

The rest of this paper is organized as follows. The discrete-time and continuous-time day-to-day models are established and examined in Sections 2 and 3, respectively. In each section, two scenarios are examined, one is when ATIS publishes the actual travel time of the previous day, and the other is when ATIS publishes the forecasted travel time which is calculated based on the travel time of the previous day. Based on the results from Sections 2 and 3, Section 4 discusses the impact of ATIS's travel time forecast on the system stability. Section 5 uses numerical examples to verify the theoretical findings and study other features of the models. Conclusions are drawn in Section 6 with discussions on possible future research directions.

[2] Hereafter in this paper, the "stability" and "local stability" both refer to "local asymptotic stability", and the "stable" and "locally stable" both refer to "locally asymptotically stable". The definition is given in Appendix A.

2. The discrete-time day-to-day models

Consider a directed traffic network with a set of directed links and a set W of origin-destination (OD) pairs. Each OD pair $w \in W$ has a fixed travel demand d_w and is connected by a set R_w of paths. Let f_{rw} be the flow on path $r \in R_w$ between OD pair $w \in W$ and $f = \left(f_{rw}, r \in R_w, w \in W \right)^{\mathrm{T}}$ the path flow vector, where 'T' represents the transpose operation. Denote $c_{rw}\left(f \right)$ as the actual travel time of path $r \in R_w$, $w \in W$, under path flow f, and $c\left(f \right) = \left(c_{rw}\left(f \right), r \in R_w, w \in W \right)^{\mathrm{T}}$.

Assume that, at day n, travelers have their own perception or prediction on the travel time of each path $r \in R_w$, $w \in W$, denoted by $p_{rw}\left(n \right)$. And before making route choices at day $n+1$, they will receive some travel time information from ATIS, which is denoted by $C_{rw}\left(n+1 \right)$ for each path $r \in R_w$, $w \in W$. Travelers will then learn and form their new perception/prediction for the imminent travel, via a learning process. A widely-used form is that travelers' new perception is a linear combination of their old perception and the travel time information from ATIS, given a learning parameter η:

$$p\left(n+1 \right) = \eta C\left(n+1 \right) + \left(1-\eta \right) p\left(n \right), \quad 0 < \eta \le 1 \tag{1}$$

where $p\left(n \right) = \left(p_{rw}\left(n \right), r \in R_w, w \in W \right)^{\mathrm{T}}$ and $C\left(n+1 \right) = \left(C_{rw}\left(n+1 \right), r \in R_w, w \in W \right)^{\mathrm{T}}$. $\eta = 1$ means $p\left(n+1 \right) = C\left(n+1 \right)$, i.e., travelers are taking ATIS's information as their new perception/prediction.

Based on the updated perception/prediction, travelers will reconsider their route choices, causing the path flows to change at the aggregate level. Assume that a certain proportion (say α) of travelers will reconsider their route choices and the resultant flow pattern follows some network loading model, while the remaining travelers would stick to their choice on the previous day. Then the flow pattern on day $n+1$ will be

$$f\left(n+1 \right) = \alpha \Phi\left(p\left(n+1 \right) \right) + \left(1-\alpha \right) f\left(n \right), \quad 0 < \alpha \le 1 \tag{2}$$

where $\Phi(\cdot)=\left(d_w\phi_{rw}(\cdot), r\in R_w, w\in W\right)^{\mathrm{T}}$ are the (stochastic) network loading functions, and $\phi_{rw}(\cdot)$ is the probability function of choosing route $r\in R_w$, $w\in W$. Hereafter, we call α the flow adjustment parameter.

Model (1)+(2) describes a day-to-day process where travelers update their perceived/predicted travel time based on the information from ATIS, and the path flows evolve according to travelers' cognitive behavior. Various types of information can be provided by ATIS, such as the actual travel time of the previous day, or some forecast based on either linear combination or more sophisticated rules. These different types of information can influence the evolution of the flows and the stability of the transportation systems, which will be discussed in the following subsections.

2.1. When ATIS publishes actual travel time of the previous day

First, we assume that ATIS publishes the actual travel time of the previous day, i.e., $C(n+1)=c(n)$, then travelers' learning process in Eq. (1) reads

$$p(n+1)=\eta c(n)+(1-\eta)p(n),\quad 0<\eta\le 1 \tag{3}$$

Model (2)+(3) is a widely-used day-to-day model (Cantarella and Cascetta, 1995; Cascetta and Cantarella, 1993) which describes the flow evolution of a network where travelers learn the travel time via exponential smoothing based on the historical travel condition and make route choices based on their perception. Its fixed points satisfy

$$p=c,\quad f=\Phi(p)$$

which coincide with the user equilibrium associated with the particular network loading function $\Phi(\cdot)$.

To judge the local stability (defined in Definition A1 in Appendix A) of each equilibrium point of the dynamical system (2)+(3) as well as other day-to-day models that will be studied later in this paper, we adopt the following two assumptions.

Assumption 1. The Jacobian of the path travel time function $c(f)$ w.r.t. the path flow vector f is symmetric and positive semidefinite.

Assumption 2. The Jacobian of the network loading function $\Phi(p)$ w.r.t. travelers' perceived travel time p is symmetric and negative semidefinite.

Remark 1. Assumption 1 naturally holds if the link travel time functions are separable, differentiable, increasing and additive (i.e., the path travel time is equal to the sum of travel time on all links that constitute the path). Assumption 2 is satisfied if the route choice probability functions $\phi_{rw}(\cdot)$ are based on the random utility theory in which the probability density functions of the perception errors do not depend on the systematic utilities (Cantarella and Cascetta, 1995), e.g., if $\phi_{rw}(\cdot)$ follow the logit model. □

We then have the following lemma which is essential for analyzing the local stability of our day-to-day models in this paper.

Lemma 1. *Denote J_f^c as the Jacobian of $c(f)$ w.r.t. f, and J_p^Φ the Jacobian of $\Phi(p)$ w.r.t. p, both evaluated at a particular equilibrium point given $c(f)$ and $\Phi(p)$. If Assumption 1 and Assumption 2 hold, then all the eigenvalues of $J_p^\Phi J_f^c$, denoted by μ_i, $i=1,2,\cdots,N$, are real and nonpositive, where N denotes the total number of paths in the network.*

Proof. The lemma is readily proved according to Theorem 7.5 in Zhang (2011) that the eigenvalues of the product of two positive semidefinite matrices are real and nonnegative. □

The following theorem then gives the stability condition of model (2)+(3).

Theorem 1. *Denote $\mu_{\min}$ as the minimum eigenvalue of $J_p^\Phi J_f^c$, i.e., $\mu_{\min} := \min_{i=1,2,\cdots,N} \mu_i$. Under Assumption 1 and Assumption 2, an equilibrium point of the discrete-time day-to-day model (2)+(3) is locally asymptotically stable if*

$$\mu_{\min} > -\frac{(2-\alpha)(2-\eta)}{\alpha\eta} = -2\frac{(1-\alpha)+(1-\eta)}{\alpha\eta} - 1 \tag{4}$$

and unstable if the inequality in Eq. (4) is reversed.

Proof. The same result has been presented in Eq. (2.27) of Cantarella and Cascetta (1995) with part of the original proof given by Cantarella and Cascetta (1994). However, as the proof in Cantarella and Cascetta (1994) is generally inaccessible both online and offline, we provide a complete proof in Appendix B. □

From Eq. (4), the local stability of an equilibrium point is determined by the minimum eigenvalue of $J_p^{\Phi} J_f^c$. Then we immediately have the following corollary regarding the stability region of an equilibrium point.

Corollary 1. *For the discrete-time model (2)+(3), when ATIS publishes actual travel time:*

(a) If $\mu_{\min} > -1$, *the equilibrium point is stable regardless of the values of the flow adjustment parameter* α *and travelers' learning parameter* η.

(b) If $\mu_{\min} \le -1$, *the equilibrium point is conditionally stable. Given* $\mu_{\min}$, *the equilibrium point is stable when*

$$\eta < \frac{2(1-\alpha)+2}{2-\alpha(\mu_{\min}+1)} \tag{5}$$

The stable and unstable regions are separated by the curve

$$\eta = \frac{4-2\alpha}{2-\alpha(\mu_{\min}+1)} \tag{6}$$

which is decreasing and convex w.r.t. α. *Here the stable (unstable) region refers to the region of* α *and* η *which makes the equilibrium point stable (unstable).*

(c) Given $\mu_{\min}$, *if an equilibrium point is stable under* $\alpha = \alpha_0$ *and* $\eta = \eta_0$, *then it is also stable under any combinations of* α *and* η *which satisfy* $\alpha \le \alpha_0$ *and* $\eta \le \eta_0$.

(d) When $\mu_{\min}$ *increases within* $(-\infty, -1]$, *the stable region w.r.t.* α *and* η *will expand.*

Proof. As the right hand side of Eq. (4) is increasing w.r.t. α and η, its maximum value is achieved at $\alpha = \eta = 1$ and equal to -1. This leads to part (a). Transforming Eq. (4) yields Eq. (5), which leads to part (b) and further part (c). Part (d) can be easily derived according to Eq. (4). □

According to Eqs. (5) and (6), the stable and unstable regions w.r.t. the flow adjustment parameter α and travelers' learning parameter η under different values of μ_{min} are illustrated in Figure 1, which verifies Corollary 1.

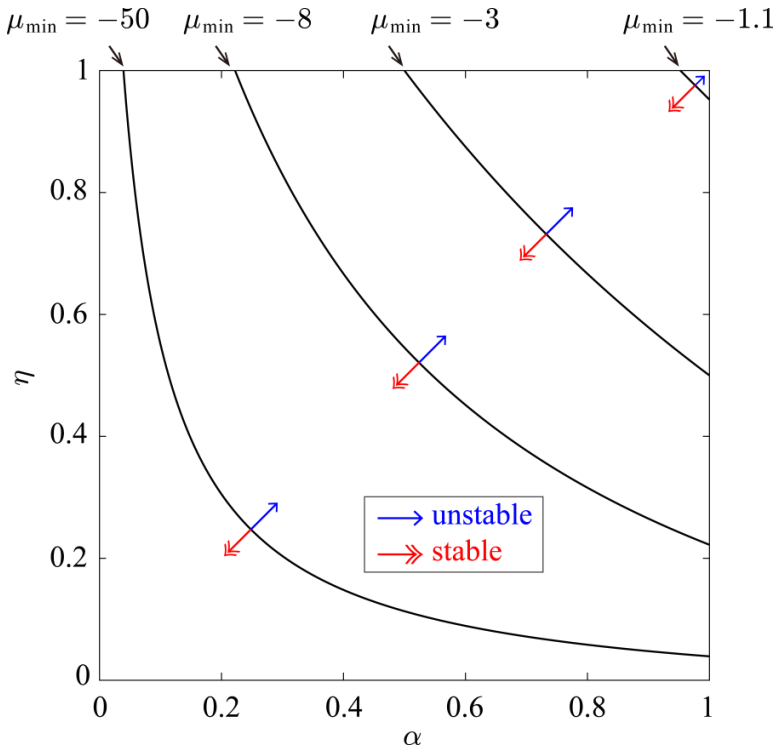

Figure 1. Stable and unstable regions of the discrete-time model when ATIS publishes actual travel time: the region on the lower-left (upper-right) of each curve is stable (unstable), while the stability under the parameter combinations on the curves is unclear.

Remark 2. In Ye et al. (2018), Eq. (3) was reformulated as

$$p(n+1) = p(n) + \eta\left[c(n) - p(n)\right], \quad 0 < \eta \le 1 \tag{7}$$

and interpreted as "travelers will correct their previous perception/prediction by adding or subtracting a proportion η of the difference between actual and perceived/predicted travel time", where η indicates the level of aggressiveness while travelers are learning the travel time. In this sense, $\eta > 1$ is also possible. Therefore, we can formulate a more general

learning model as

$$p(n+1)=\max\left\{p(n)+\eta\left[c(n)-p(n)\right],0\right\},\ \ \eta>0 \tag{8}$$

where the function $\max\{\cdot,0\}$ avoids negative values of perception/prediction but will not affect the analysis on the local stability if the travel time functions of all links are strictly positive (so the equilibrium path travel time will be strictly positive). In this case, Theorem 1 will still be valid for judging the local stability of the new system (8)+(2), which is explained in Remark 4 in Appendix B. □

2.2. When ATIS publishes forecasted travel time

Now we consider another case when ATIS adopts a more proactive strategy and publishes the forecasted travel time by learning from the actual travel time of the previous day. The new forecast is calculated as a linear combination of the old forecast and the actual travel time of the previous day:

$$C(n+1)=\theta c(n)+(1-\theta)C(n),\ \ 0<\theta\le 1 \tag{9}$$

where θ is ATIS's forecasting parameter. Model (9)+(1)+(2) now describes the day-to-day dynamic when both ATIS and travelers are learning. Notably, when $\theta=1$, we have $C(n+1)=c(n)$ and the dynamic degenerates to model (2)+(3).

The fixed points of model (9)+(1)+(2) also coincide with the user equilibrium under the network loading function $\Phi(\cdot)$. Local stability of the fixed points can be checked via Theorem 2 below.

Theorem 2. *Denote*

$$a_i=-\left[(1-\alpha)+(1-\theta)+(1-\eta)+\alpha\theta\eta\mu_i\right] \tag{10}$$

$$h=(1-\alpha)(1-\theta)+(1-\theta)(1-\eta)+(1-\eta)(1-\alpha) \tag{11}$$

$$g=-(1-\alpha)(1-\theta)(1-\eta) \tag{12}$$

$$\Delta_0(\mu_i)=18a_ihg-4a_i^3g+a_i^2h^2-4h^3-27g^2 \tag{13}$$

$$\tilde{\Delta}(\mu_i) = a_i^2 - 3h \tag{14}$$

$$\mu_- = \frac{-\sqrt{3h} - \left[(1-\alpha)+(1-\theta)+(1-\eta)\right]}{\alpha\theta\eta} \tag{15}$$

and

$$\mu_+ = \frac{\sqrt{3h} - \left[(1-\alpha)+(1-\theta)+(1-\eta)\right]}{\alpha\theta\eta} \tag{16}$$

- *When* $\max\{\alpha,\theta,\eta\} = 1$, *an equilibrium point is asymptotically stable if*

$$\mu_{\min} > -\frac{(2-\alpha)(2-\theta)(2-\eta)}{\alpha\theta\eta} \tag{17}$$

  and unstable if the inequality in Eq. (17) is reversed.

- *When* $\max\{\alpha,\theta,\eta\} < 1$, *an equilibrium point is*

  - *asymptotically stable if each* μ_i, $i = 1, 2, \cdots, N$, *satisfies one of the following three conditions:*

    (i) $\tilde{\Delta}(\mu_i) \le 0$, *i.e.,* $\mu_- \le \mu_i \le \mu_+$.

    (ii) $\tilde{\Delta}(\mu_i) > 0$ *(i.e.,* $\mu_i < \mu_-$ *or* $\mu_i > \mu_+$*),* $\Delta_0(\mu_i) < 0$ *and*

$$\mu_i > \frac{\left[(1-\alpha)(1-\theta)-1\right]\left[(1-\theta)(1-\eta)-1\right]\left[(1-\eta)(1-\alpha)-1\right]}{\alpha\theta\eta(1-\alpha)(1-\theta)(1-\eta)} \tag{18}$$

    (iii) $\tilde{\Delta}(\mu_i) > 0$, $\Delta_0(\mu_i) \ge 0$, *and*

$$\mu_i > \max\left\{-\frac{h+3+2\left[(1-\alpha)+(1-\theta)+(1-\eta)\right]}{2\alpha\theta\eta}, -\frac{(2-\alpha)(2-\theta)(2-\eta)}{\alpha\theta\eta}\right\} \tag{19}$$

  - *unstable if at least one* μ_i, $i = 1, 2, \cdots, N$, *satisfies one of the following two conditions:*

    (iv) $\tilde{\Delta}(\mu_i) > 0$, $\Delta_0(\mu_i) < 0$, *and the inequality in Eq. (18) is reversed.*

    (v) $\tilde{\Delta}(\mu_i) > 0$, $\Delta_0(\mu_i) \ge 0$, *and the inequality in Eq. (19) is reversed.*

Proof. The proof is provided in Appendix C. □

Remark 3. In Theorem 2, when $\max\{\alpha,\theta,\eta\}\to 1$, the stability condition for $\max\{\alpha,\theta,\eta\}<1$ will degenerate to the stability condition for $\max\{\alpha,\theta,\eta\}=1$, i.e., conditions (i)-(iii) will reduce to Eq. (17), and conditions (iv)-(v) will reduce to the reverse of Eq. (17). The proof is provided in Appendix D. This agrees with the fact that when ATIS's forecasting parameter $\theta=1$, the model degenerates to the case that ATIS publishes actual travel time. □

When ATIS publishes forecasted travel time, the stability condition given by Theorem 2 is much more complex than Theorem 1. Therefore, we don't have the similar results of Corollary 1; instead, we explore the system properties numerically. Given an eigenvalue μ_i, we enumerate all the possible combinations of the three parameters α, θ and η in a resolution of 0.001, check whether the stability condition is met according to Theorem 2, and draw the stable and unstable regions under different values of μ_i in Figure 2. Here the stable (unstable) region refers to the region of α, θ and η which makes the equilibrium point stable (unstable). We then have the following observations on the plots:

(a) When $\mu_i \geq -1$, the whole feasible region of α, θ and η is the stable region.

(b) When μ_i decreases in $(-\infty,-1)$, the unstable region will expand and thus the stable region will shrink.

(c) As according to Theorem 2, the stable region for an equilibrium point will be the union of the stable regions under all eigenvalues μ_i, $i=1,2,\cdots,N$, then from (a) and (b), the stability of an equilibrium point is determined by the minimum eigenvalue $\mu_{\min}$.

(d) The intersection of the unstable region with the plane $\theta=1$ is the same as the unstable region given in Figure 1, which agrees with Remark 3.

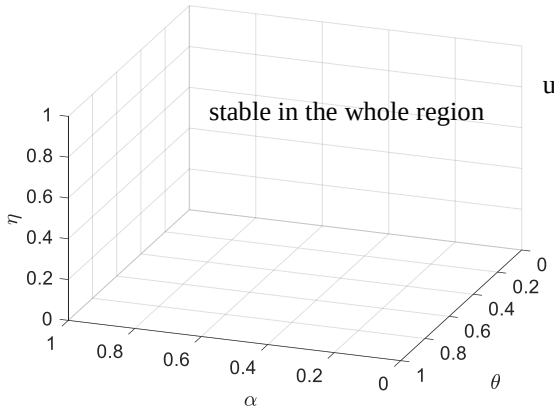

(a) $\mu_i = -1$

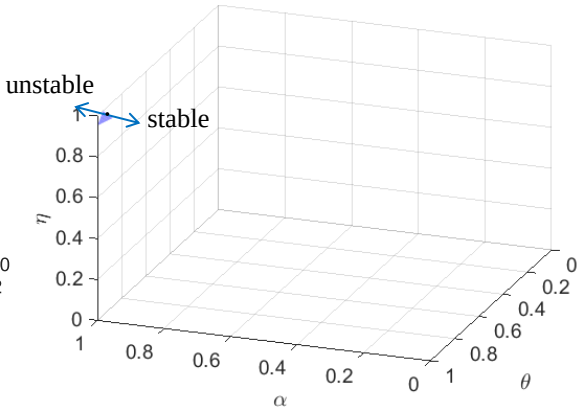

(b) $\mu_i = -1.1$

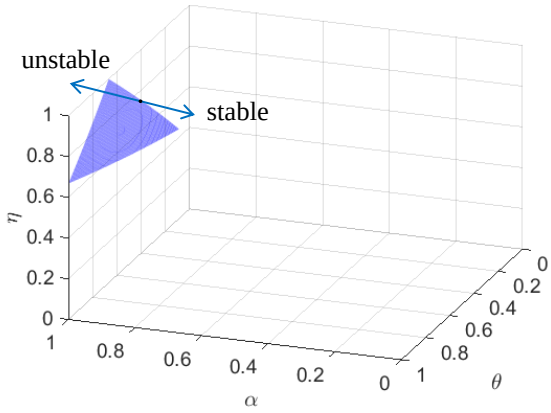

(c) $\mu_i = -2$

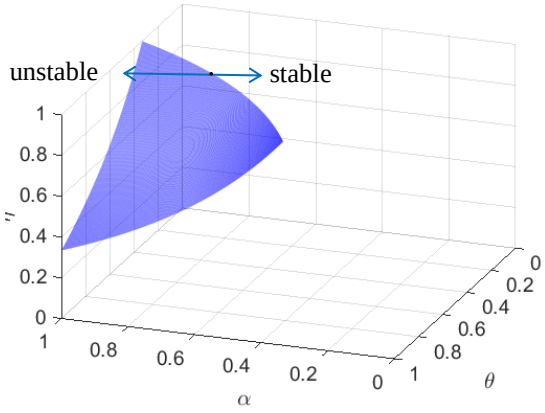

(d) $\mu_i = -5$

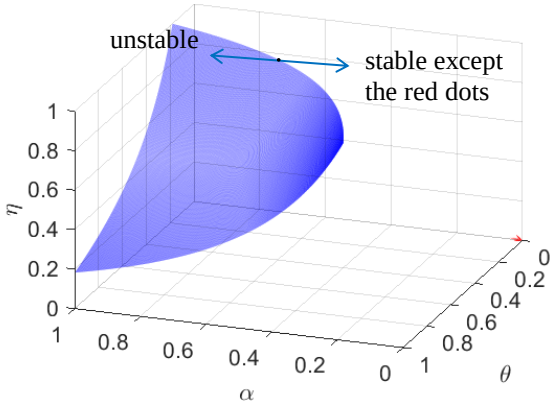

(e) $\mu_i = -10$

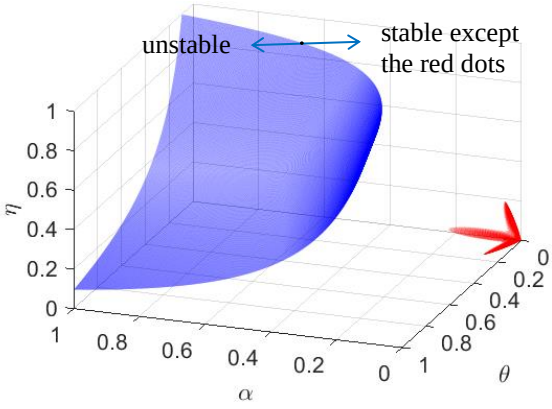

(f) $\mu_i = -20$

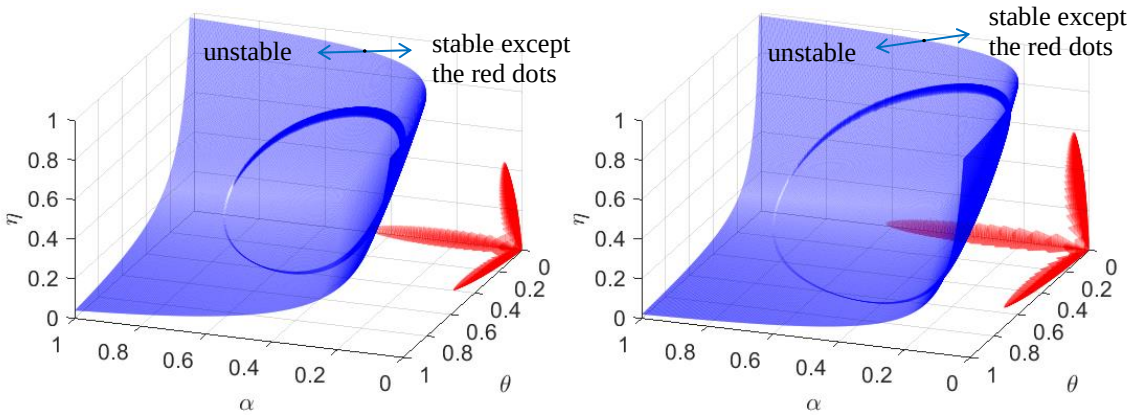

(g) $\mu_i = -50$ (h) $\mu_i = -100$

Figure 2. Stable and unstable regions of the discrete-time model w.r.t. different eigenvalues μ_i, when ATIS publishes forecasted travel time.

3. The continuous-time day-to-day models

This section reexamines the two scenarios in Section 2 using continuous-time models. To derive the corresponding continuous-time model of its discrete-time counterpart, we refer to Watling (1999) and assume that, for a day-to-day process modeled in continuous time, after a small increment of time δ, the adjustments of travelers' perceptions and path flows will be similar to Eqs. (2) and (3) but proportional to δ:

$$p(t+\delta) = \hat{\eta}\delta C(t+\delta) + (1-\hat{\eta}\delta)\, p(t), \quad \hat{\eta} > 0 \tag{20}$$

$$f(t+\delta) = \hat{\alpha}\delta\Phi\big(p(t+\delta)\big) + (1-\hat{\alpha}\delta)\, f(t), \quad \hat{\alpha} > 0 \tag{21}$$

where t represents the day which is considered to be continuous; $\hat{\eta}$ and $\hat{\alpha}$ are travelers' learning parameter and the flow adjustment parameter in the continuous-time model, respectively. When $\delta \to 0$, Eqs. (20) and (21) will lead to the following continuous-time process (22)+(23):

$$\dot{p} = \hat{\eta}\big(C - p\big), \quad \hat{\eta} > 0 \tag{22}$$

$$\dot{f} = \hat{\alpha}\big(\Phi(p) - f\big), \quad \hat{\alpha} > 0 \tag{23}$$

3.1. When ATIS publishes actual travel time of the previous day

When ATIS publishes actual travel time of the previous day, i.e., $C = c$, Eq. (22) will read

$$\dot{p} = \hat{\eta}\left(c - p\right), \quad \hat{\eta} > 0 \tag{24}$$

Then model (23)+(24) describes a continuous-time day-to-day dynamic where the ATIS publishes the actual travel time of the previous day. The local stability condition of each equilibrium state of the model is given in Theorem 3.

Theorem 3. *Under Assumption 1 and Assumption 2, all the equilibrium points of dynamic (23)+(24) are locally asymptotically stable.*

Proof. The result can be immediately derived from Theorem 1: when the time step $\delta \to 0$, $\hat{\eta}\delta \to 0$ in Eq. (20) and $\hat{\alpha}\delta \to 0$ in Eq. (21), then condition (4) becomes $\mu_{\min} > -\infty$, meaning the continuous-time system is always locally stable. But still, we can directly prove the theorem based on the formulation of the continuous-time model, and the proof is provided in Appendix E. □

3.2. When ATIS publishes forecasted travel time

When ATIS forecasts the travel time, we can assume

$$C\left(t + \delta\right) = \hat{\theta}\delta c\left(t\right) + \left(1 - \hat{\theta}\delta\right)C\left(t\right) \tag{25}$$

and obtain the continuous-time model as

$$\dot{C} = \hat{\theta}\left(c - C\right), \quad \hat{\theta} > 0 \tag{26}$$

where $\hat{\theta}$ is ATIS's forecasting parameter in the continuous-time model. When $\hat{\theta} = +\infty$, we have $c = C$ and the dynamical process (26)+(22)+(23) degenerates to model (23)+(24).

The stability condition of each fixed point of the continuous-time model (26)+(22)+(23) is established in Theorem 4 below, which cannot be directly derived from the stability condition of the corresponding discrete-time model.

Theorem 4. *Under Assumption 1 and Assumption 2, for the dynamical system (26)+(22)+(23):*

(i) If $\hat{\alpha} = \hat{\theta} = \hat{\eta}$, *the equilibrium point is stable regardless of the eigenvalues* μ_i.

(ii) If $\hat{\alpha}$, $\hat{\theta}$ *and* $\hat{\eta}$ *are not all equal, then the equilibrium point is stable if*

$$\mu_{\min} > \frac{\hat{\alpha}\hat{\theta}\hat{\eta} - \left(\hat{\alpha} + \hat{\theta} + \hat{\eta}\right)\left(\hat{\alpha}\hat{\theta} + \hat{\theta}\hat{\eta} + \hat{\eta}\hat{\alpha}\right)}{\hat{\alpha}\hat{\theta}\hat{\eta}} \tag{27}$$

and unstable if the inequality in Eq. (27) is reversed.

Proof. The proof is provided in Appendix F. □

From Theorem 4, we immediately have the following corollary.

Corollary 2. *For the continuous-time model (26)+(22)+(23):*

(a) Given the minimum eigenvalue $\mu_{\min}$, *if the equilibrium point is stable under* $\hat{\alpha} = \hat{\alpha}_0$, $\hat{\theta} = \hat{\theta}_0$ *and* $\hat{\eta} = \hat{\eta}_0$, *it is not necessarily stable under a combination of* $\hat{\alpha}$, $\hat{\theta}$ *and* $\hat{\eta}$ *which satisfy* $\hat{\alpha} \le \hat{\alpha}_0$, $\hat{\theta} \le \hat{\theta}_0$ *and* $\hat{\eta} \le \eta_0$.

(b) When $\mu_{\min} > -8$, *the equilibrium point is stable regardless of the values of* $\hat{\alpha}$, $\hat{\theta}$ *and* $\hat{\eta}$.

(c) When $\mu_{\min} \le -8$, *the equilibrium point is conditionally stable.*

(d) When $\mu_{\min}$ *decreases in* $(-\infty, -8]$, *the stable region w.r.t.* $\hat{\alpha}$, $\hat{\theta}$ *and* $\hat{\eta}$ *will shrink.*

(e) The stable and unstable regions are determined by $\hat{\alpha}/\hat{\theta}$ *and* $\hat{\eta}/\hat{\theta}$, *meaning the stability of the system will maintain when* $\hat{\alpha}$, $\hat{\theta}$ *and* $\hat{\eta}$ *all scale up or down by the same ratio.*

(f) If $\hat{\theta} = +\infty$ *and* $\max\{\hat{\alpha}, \hat{\eta}\} < +\infty$, *the equilibrium point is stable for any* $\mu_{\min} > -\infty$, *which confirms Theorem 3.*

Proof. Denote $\Omega\left(\hat{\alpha}, \hat{\theta}, \hat{\eta}\right)$ as the right hand side of Eq. (27), then

$$\frac{\partial\Omega\left(\hat{\alpha},\hat{\theta},\hat{\eta}\right)}{\partial\hat{\eta}}=-\frac{\hat{\alpha}+\hat{\theta}}{\hat{\alpha}\hat{\theta}}\frac{\hat{\eta}^2-\hat{\alpha}\hat{\theta}}{\hat{\eta}^2}$$

Therefore, $\Omega\left(\hat{\alpha},\hat{\theta},\hat{\eta}\right)$ is not monotonic w.r.t. $\hat{\eta}$, and thus part (a) holds. Further, given $\hat{\alpha}$ and $\hat{\theta}$, $\frac{\partial\Omega}{\partial\hat{\eta}}>0$ if $\hat{\eta}<\sqrt{\hat{\alpha}\hat{\theta}}$, and $\frac{\partial\Omega}{\partial\hat{\eta}}<0$ if $\hat{\eta}>\sqrt{\hat{\alpha}\hat{\theta}}$, so Ω achieves the maximum at $\hat{\eta}=\sqrt{\hat{\alpha}\hat{\theta}}$. Since $\Omega\left(\hat{\alpha},\hat{\theta},\hat{\eta}\right)$ is symmetric w.r.t. $\hat{\alpha}$, $\hat{\theta}$ and $\hat{\eta}$, then $\Omega\left(\hat{\alpha},\hat{\theta},\hat{\eta}\right)$ has a maximum equal to -8 achieved when $\hat{\alpha}=\hat{\theta}=\hat{\eta}$. Hence parts (b) and (c) hold. Part (d) is obtained according to Eq. (27) and part (b).

Further in Eq. (27), dividing $\hat{\theta}^3$ in both the numerator and denominator of the right hand side and letting $\tilde{\alpha}=\hat{\alpha}/\hat{\theta}$ and $\tilde{\eta}=\hat{\eta}/\hat{\theta}$, we have

$$\mu_{\min}>\frac{\tilde{\alpha}\tilde{\eta}-\left(\tilde{\alpha}+\tilde{\eta}+1\right)\left(\tilde{\alpha}+\tilde{\eta}+\tilde{\alpha}\tilde{\eta}\right)}{\tilde{\alpha}\tilde{\eta}} \tag{28}$$

which yields part (e).

For part (f), when $\hat{\theta}=+\infty$ and $\max\left\{\hat{\alpha},\hat{\eta}\right\}<+\infty$, the right hand side of Eq. (27) is equal to

$$\frac{\hat{\alpha}\hat{\eta}-\left(\frac{\hat{\alpha}}{\hat{\theta}}+1+\frac{\hat{\eta}}{\hat{\theta}}\right)\left(\hat{\alpha}\hat{\theta}+\hat{\theta}\hat{\eta}+\hat{\eta}\hat{\alpha}\right)}{\hat{\alpha}\hat{\eta}}=-\infty$$

Thus Eq. (27) holds if $\mu_{\min}>-\infty$. It means when $\hat{\theta}=+\infty$ (i.e., ATIS publishes actual travel time), the equilibrium points of the continuous-time system are always asymptotically stable, which agrees with Theorem 3. □

Based on Eq. (28), the stable and unstable regions under different values of $\mu_{\min}$ are plotted in Figure 3, which verifies Corollary 2.

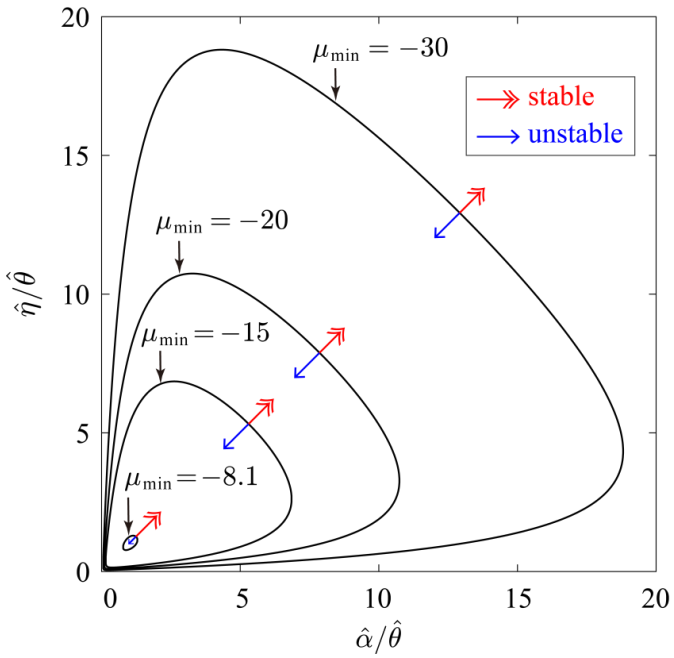

Figure 3. Stable and unstable regions of the continuous-time model when ATIS publishes forecasted travel time: the region inside (outside) each curve is unstable (stable), while the stability under the parameter combinations on the curves is unclear.

4. Impact of ATIS's forecasting behavior on system stability

Theorems 1-4 have examined how the parameters of the day-to-day models determine the stability of the discrete-time and continuous-time models. From these results, we can investigate the impact of different types of information on the system stability, and compare the conclusions drawn based on the discrete-time and continuous-time models.

Conclusions based on the continuous-time models can be directly drawn according to Theorem 3 and Theorem 4: if the ATIS publishes the actual historical travel time, the equilibrium points are always locally asymptotically stable; when ATIS forecasts the travel time via the exponential-smoothing learning rule, the equilibrium points will have a chance to be unstable. It means ATIS's proactive forecasting strategy reduces the stability of the system.

When using the discrete-time models, similar comparisons cannot be made between Theorem 1 and Theorem 2, due to the complex stability condition given in Theorem 2. However, Figure 2 shows that ATIS's forecasting makes the system behavior more complex, compared with the case when ATIS does not forecast. The findings are summarized as follows.

- Comparing Figure 2(a)(b), when the minimum eigenvalue $\mu_{\min} > \mu^{c1}$, where μ^{c1} is a critical value which is approximately -1, the system is always stable no matter ATIS forecasts the travel time or not, so ATIS's strategy has no impact on the system stability.
- Comparing Figure 2(b)(c)(d)(e), when $\mu^{c2} < \mu_{\min} < \mu^{c1}$, where μ^{c2} is another critical value probably between -5 and -10, a smaller θ (weight on the historical travel time) corresponds to a smaller unstable region of α and η. This means ATIS's forecasting behavior ($\theta < 1$) enlarges the stable region, compared with the case when ATIS publishes the historical travel time ($\theta = 1$).
- Comparing Figure 2(e)(f)(g)(h), when $\mu_{\min} < \mu^{c2}$, the situation is more complex: a combination of the flow adjustment parameter α and travelers' learning parameter η which is stable (unstable) when the actual travel time is published can become unstable (stable) if the forecasted travel time is published.

In summary, the discrete-time modeling concludes that, compared with the case when ATIS publishes actual historical travel time, publishing the forecasted travel time will either (i) expand the stability region and thus improve the system stability, or (ii) reverse the stability for some combinations of the system parameters.

Overall, we may conclude that, the conclusions drawn from the discrete-time modeling and continuous-time modeling can be consistent, different or contradictory, which depends on the system parameters α, θ, η and the eigenvalues μ_i. And compared with the continuous-time models, the discrete-time models behave in a more complex manner and do not always favor ATIS's forecasting behavior from the perspective of system stability.

5. Numerical example

In this section, we use a simple network (thus the eigenvalues μ_i are fixed) to test and verify the theoretical results in the previous sections, and further discuss some system features that were not theoretically discussed, in particular, how ATIS's forecast influences the evolution of flows.

The Braess network (Figure 4) with only one OD pair is chosen as the example network. A

fixed demand of 10 is served by three paths (Path 1, O→1→3→D; Path 2, O→2→4→D; Path 3, O→2→5→3→D). The travel time $c_j(v_j)$ on each link j is determined by $c_j(v_j) = c_j^0\left[1+(v_j/Y_j)^4\right]$, where v_j is the link flow, and c_j^0 and Y_j are parameters given in Table 1.

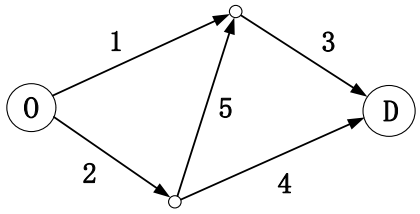

Figure 4. The Braess network.

Table 1. Parameters of the link travel time functions in the Braess network

Link index j	1	2	3	4	5
c_j^0	2	2	1	2	1
Y_j	4	7	7	3	3

The route choice probabilities are assumed to follow the logit model, i.e.,

$$\phi_{rw}(p) = \frac{\exp(-\beta p_{rw})}{\sum_{i\in R_w}\exp(-\beta p_{iw})}, \quad r \in R_w, \quad w \in W$$

We set $\beta = 5$, so the equilibrium path flow pattern is uniquely $[5.2824,\ 2.6236,\ 2.094]^{\mathrm{T}}$, and the equilibrium path travel time pattern is $[4.0974,\ 4.2374,\ 4.2825]^{\mathrm{T}}$. Therefore, the three eigenvalues of $J_p^{\Phi}J_f^c$ evaluated at the equilibrium point are $\mu_1 = 0$, $\mu_2 = -2.280$ and $\mu_3 = -11.105$.

The primary objective of this numerical example is to check the stability of the established models and show that the models behave the same as the theories predict. To do so, we examine the trajectories of path flows under different combinations of parameters. As we are investigating the local stability, we assume that the initial path flow pattern is slightly perturbed from the equilibrium flow pattern and equal to $[5.3,\ 2.6,\ 2.1]^{\mathrm{T}}$, and that the initial

travel time patterns predicted by the travelers and forecasted by the ATIS are both equal to the equilibrium path travel time.

5.1. The discrete-time models

For the case when ATIS publishes actual travel time, we set travelers' learning parameter $\eta = 0.5$. Then according to Theorem 1 and Corollary 1, the equilibrium is stable when the flow adjustment parameter $\alpha < 0.425$ and unstable when $\alpha > 0.425$. To verify this, Figure 5 displays the flow trajectories when α is 0.424 and 0.426, respectively; as expected, the former is stable and the latter is not. Since the feasible path flow patterns have to meet the flow conservation constraint due to the fixed demand, we only display the flows on Paths 1 and 2.

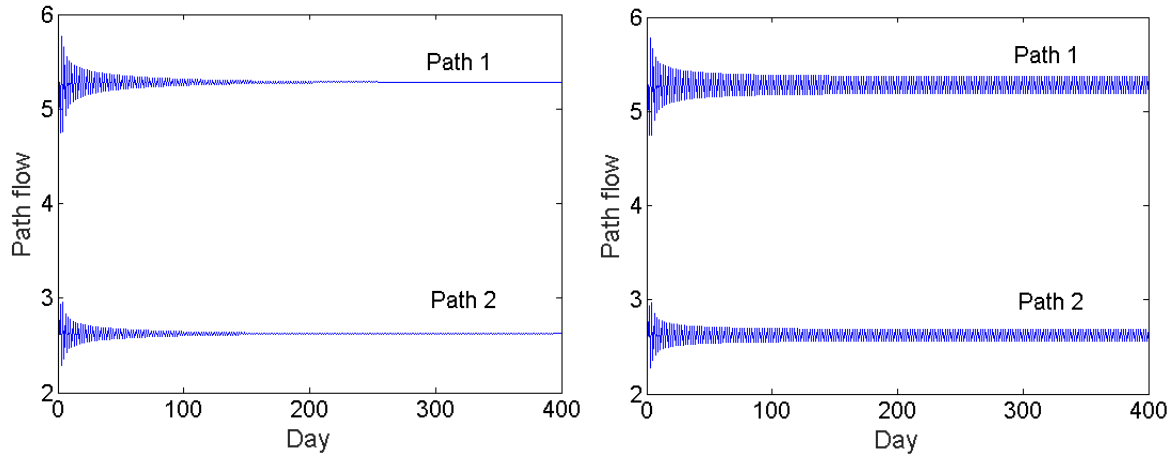

(a) $\alpha = 0.424$ (b) $\alpha = 0.426$

Figure 5. Flow trajectories of the discrete-time model under different flow adjustment parameter α, when ATIS publishes actual travel time.

When ATIS publishes forecasted travel time, we set travelers' learning parameter $\eta = 0.5$ and ATIS's forecasting parameter $\theta = 0.6$. According to Theorem 2, the system is stable when flow adjustment parameter $\alpha < 0.773$ and unstable when $\alpha > 0.773$. To verify this, Figure 6 shows the flow trajectories when α is 0.772 and 0.774, respectively; as expected, the former is stable and the latter is not.

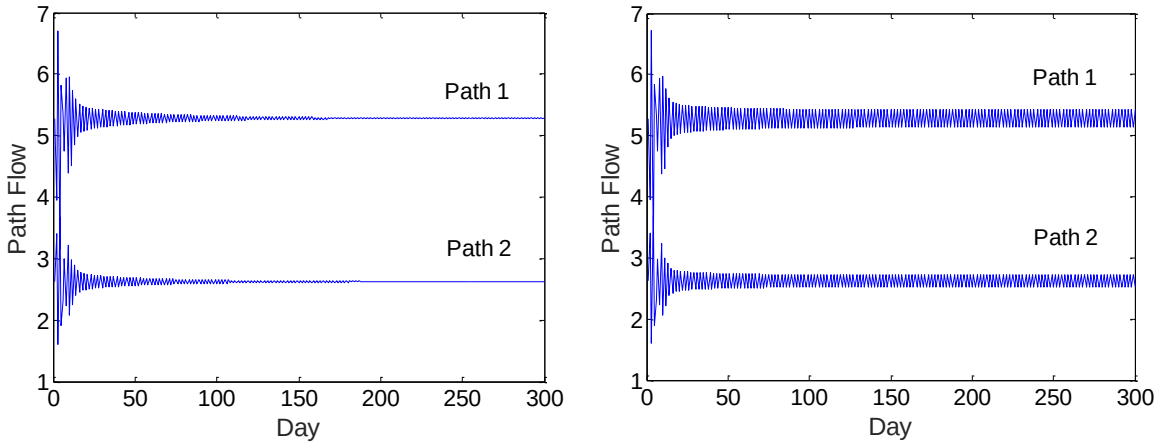

(a) $\alpha = 0.772$ (b) $\alpha = 0.774$

Figure 6. Flow trajectories of the discrete-time model under different flow adjustment parameter α, when ATIS publishes forecasted travel time.

5.2. The continuous-time models

This subsection investigates the stability of the continuous-time models. Since when ATIS publishes actual travel time, the equilibrium is always stable, we only look into the case when ATIS publishes forecasted travel time. Here we choose the flow adjustment parameter $\hat{\alpha} = 2$ and travelers' learning parameter $\hat{\eta} = 3$. According to Theorem 4 and Corollary 2, the equilibrium point is stable when ATIS's forecasting parameter $\hat{\theta} < 0.80$ or $\hat{\theta} > 7.53$, and unstable when $0.80 < \hat{\theta} < 7.53$. To verify, we plot the flow trajectories under different values of $\hat{\theta}$ in Figure 7. To obtain the flow trajectories, the ordinary differential equation sets which describe the day-to-day dynamics are solved numerically by MATLAB's built-in function *ode45* which employs the fourth-order Runge-Kutta method.

Figure 7 shows the trajectories of flow on Path 1 when $\hat{\theta}$ varies. The blue dashed (red solid) lines are the trajectories when ATIS publishes actual (forecasted) travel time. The findings are summarized as follows.

(i) When ATIS publishes actual travel time, the day-to-day process is stable and convergent.

(ii) When $\hat{\theta}$ is very small, e.g. 0.02 in Figure 7(a), the flow converges with minimum fluctuation. As $\hat{\theta}$ increases in the stable region ($\hat{\theta} < 0.80$, Figure 7(a)(b)(c)), the flow fluctuates more and more but still converges.

(iii) When $\hat{\theta}$ enters the unstable region (i.e., $0.80 < \hat{\theta} < 7.53$, Figure 7(d)(e)), the flow fluctuates without converging.

(iv) When $\hat{\theta}$ further increases and re-enters the stable region ($\hat{\theta} > 7.53$, Figure 7(f)(g)), the system goes back to stabilization, and the flow fluctuates less as $\hat{\theta}$ increases.

(v) When $\hat{\theta}$ is very large, e.g. 100.00 in Figure 7(g), the trajectory almost overlaps with that when ATIS publishes actual travel time; this is consistent with the theory that when $\hat{\theta} \to +\infty$, the system degenerates to the case of publishing actual travel time.

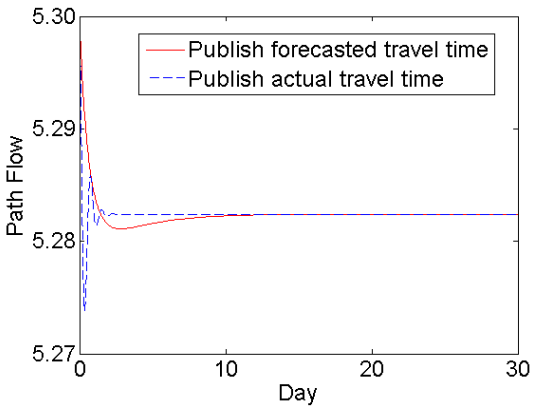

(a) $\hat{\theta} = 0.02$

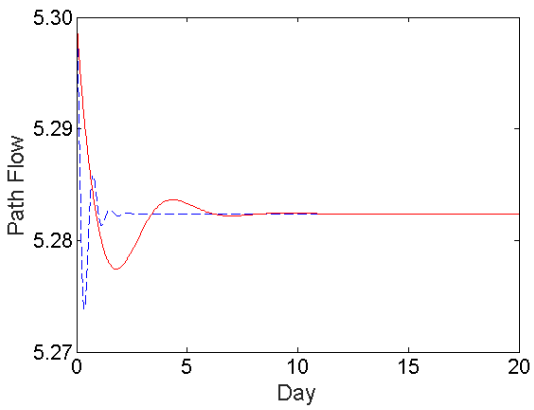

(b) $\hat{\theta} = 0.10$

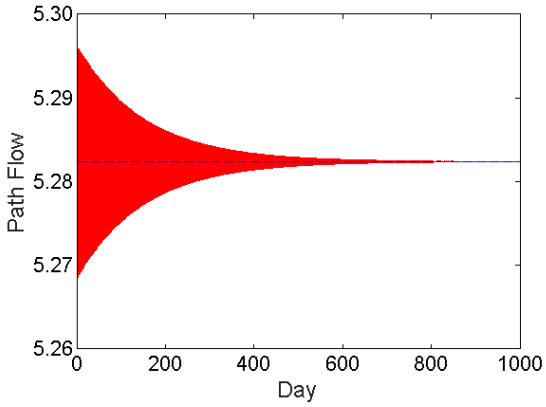

(c) $\hat{\theta} = 0.78$

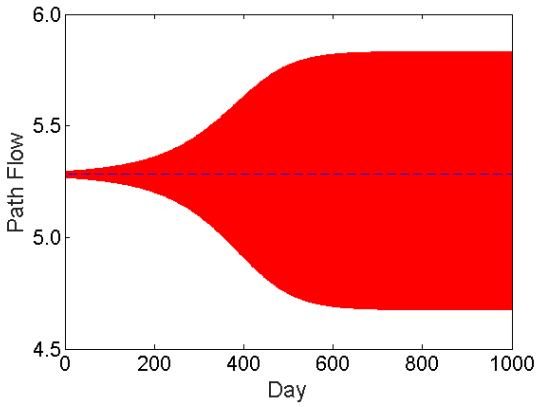

(d) $\hat{\theta} = 0.82$

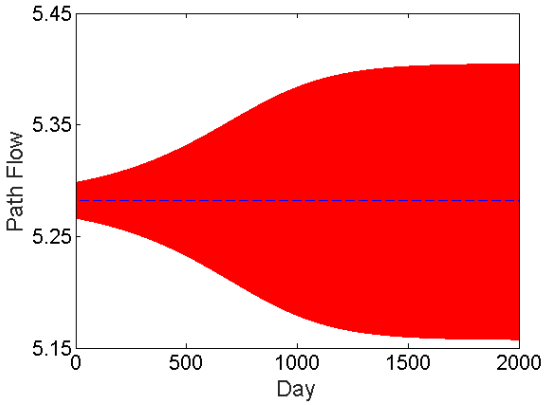

(e) $\hat{\theta} = 7.50$

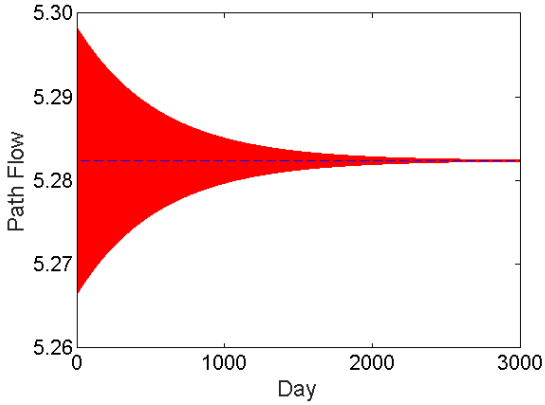

(f) $\hat{\theta} = 7.55$

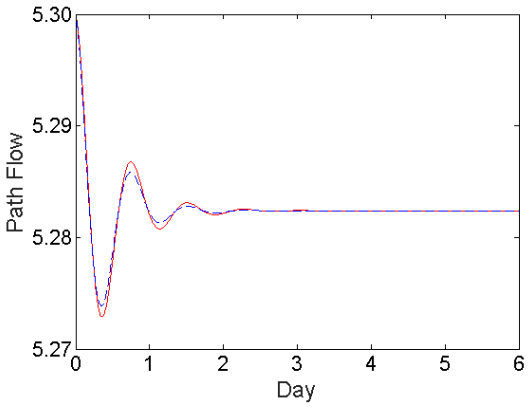

(g) $\hat{\theta} = 100.00$

Figure 7. Evolution of flow on Path 1 under different values of ATIS's forecasting parameter $\hat{\theta}$: blue dashed lines for publishing actual travel time, and red solid lines for publishing forecasted travel time.

6. Conclusions

This paper employs several discrete-time and continuous-time dynamical models to study the day-to-day evolution of traffic flows in a road network where travelers receive information from ATIS, form their own prediction/perception on travel time, and then choose routes. The discrete-time model when ATIS publishes actual travel time of the previous day (called the "ATIS-A" scenario) is first examined, which is the same model as that in Cantarella and Cascetta (1995). Then the second discrete-time model is analyzed for the case when ATIS

publishes the forecasted travel time obtained by exponential-smoothing learning (called the "ATIS-F" scenario). After this, the continuous-time models are used to reinvestigate the ATIS-A and ATIS-F scenarios.

We derive the stability conditions of the discrete-time and continuous-time dynamics for both ATIS-A and ATIS-F scenarios.

- For the discrete-time models, the stability of both ATIS-A and ATIS-F depends on the eigenvalues associated with travel time functions and network loading functions, and on the system parameters. Changing the system from ATIS-A to ATIS-F will change the system stability in the following two different directions, depending on the above-mentioned eigenvalues and system parameters:
  - the stability region will maintain or expand, meaning ATIS's forecast will maintain or improve the system stability; or
  - some combinations of the system parameters which are unstable (stable) under ATIS-A will become stable (unstable) under ATIS-F.
- For the continuous-time models, the ATIS-A system is always stable, and the ATIS-F case can be unstable under certain combinations of parameters. It means ATIS's forecast will reduce the system stability.

Therefore, conclusions drawn from the discrete-time models are more complex than or even contrary to that from the continuous-time models. This implies that, when comparing the stability of two day-to-day processes, the discrete-time and continuous-time models can lead to different conclusions.

For future research, following the idea in this paper, we can introduce ATIS's forecast to other day-to-day processes such as those in Smith (1984), Friesz et al. (1994), Nagurney and Zhang (1997), Smith and Watling (2016) and Yang and Zhang (2009). On the other hand, this paper only examines the system stability under a particular forecasting rule of ATIS. In the future, it is also interesting and meaningful to investigate how ATIS's forecasting algorithms and information releasing strategies affect the system performance in terms of equilibrium state, stability, convergence speed, oscillation, cumulative travel time and so on. Moreover, travelers' compliance rate to ATIS may change with the accuracy of the travel time forecast, which can also be considered in the day-to-day models, while the challenge is to maintain the mathematical tractability of the model for stability analysis. Finally, as the travel time forecast is more widely used for short-term forecast in a within-day context, it is also worth

investigating a combined day-to-day and within-day model under ATIS, where the departure time can be either predetermined (as in Mounce and Carey, 2011; Zhang et al., 2001) or adjustable on each day (as in Cascetta and Cantarella, 1991; Yu et al., 2020).

Acknowledgements. The authors wish to express their thanks to the anonymous reviewers for their useful comments on the early versions of this paper. The work described in this paper was supported by grants from The National Natural Science Foundation of China under project no. 72025104, 71861167001 and Hong Kong Research Grants Council under project HKUST16211114.

Appendix A. Stability theorems

Definition A1. (Definition 4.1, Khalil, 2002) *Suppose* x^* *is an equilibrium point of the autonomous system*

$$\dot{x} = \Psi(x) \tag{29}$$

where $\Psi : M \to \mathbb{R}^m$ *is a locally Lipschitz map from a domain* $M \subset \mathbb{R}^m$ *into* $\mathbb{R}^m$. *The equilibrium point is*

- *locally stable if for each* $\varepsilon > 0$, *there is* $\xi = \xi(\varepsilon) > 0$ *such that*

$$\|x(0) - x^*\| < \xi \Rightarrow \|x(t) - x^*\| < \varepsilon, \quad \forall t \geq 0;$$

- *unstable if it is not stable; and*
- *locally asymptotically stable if it is stable and* ξ *can be chosen such that*

$$\|x(0) - x^*\| < \xi \Rightarrow \lim_{t \to \infty} \|x(t) - x^*\| = 0$$

where $\|x\|$ *stands for the norm of vector* x.

The local stability of a discrete-time system

$$x(n+1) = \Psi(x(n)) \tag{30}$$

can be defined in a similar way. For simplicity, the rigorous definition is not presented here.

The local stability of systems (29) and (30) can be analyzed via linearization as given by the

following theorem.

Theorem A1. (Theorem 4.7, Khalil, 2002; Theorems 9.1.2, 9.1.3, Lebovitz, n.d.) *Let* x^* *be an equilibrium point for the system (29) or (30) where* $\Psi : M \to \mathbb{R}^m$ *is continuously differentiable and* M *is a neighborhood of* x^*. *Let*

$$J = \left.\frac{\partial \Psi(x)}{\partial x}\right|_{x=x^*}$$

For system (29), x^* *is*

- *locally asymptotically stable if the real parts of all the eigenvalues of* J *are negative; and*
- *unstable if the real part of at least one of the eigenvalues of* J *is positive.*

For system (30), x^* *is*

- *locally asymptotically stable if the moduli (i.e., absolute values) of all the eigenvalues of* J *are less than 1; and*
- *unstable if the modulus of at least one of the eigenvalues of* J *is greater than 1*.

The following theorems are also used in the subsequent proofs.

Theorem A2. (adopted from Eq. 0.8.5.13 in Horn and John, 2013) *For block matrices* A_{11}, A_{12}, A_{21} *and* A_{22}, *if* A_{11} *and* A_{12} *commute, i.e.,* $A_{11}A_{12} = A_{12}A_{11}$, *then*

$$\begin{vmatrix} A_{11} & A_{12} \\ A_{21} & A_{22} \end{vmatrix} = |A_{11}A_{22} - A_{21}A_{12}|$$

Theorem A3. (adopted from Eq. 0.8.5.3 in Horn and John, 2013) *For block matrices* A_{11}, A_{12}, A_{21} *and* A_{22}, *if* A_{11} *is invertible, then* $\begin{vmatrix} A_{11} & A_{12} \\ A_{21} & A_{22} \end{vmatrix} = |A_{11}||A_{22} - A_{21}A_{11}^{-1}A_{12}|$.

Appendix B. Proof of Theorem 1

The Jacobian matrix of dynamical system (3)+(2) at the equilibrium point is calculated as

$$J_1 = \begin{pmatrix} (1-\eta) I & \eta J_f^c \\ \alpha(1-\eta) J_p^{\Phi} & \alpha\eta J_p^{\Phi} J_f^c + (1-\alpha) I \end{pmatrix} \tag{31}$$

The eigenvalues of J_1, denoted by λ, are the roots of the following equation:

$$\left|\lambda I - J_1\right| = \begin{vmatrix} \left[\lambda - (1-\eta)\right] I & -\eta J_f^c \\ -\alpha(1-\eta) J_p^{\Phi} & \left[\lambda - (1-\alpha)\right] I - \alpha\eta J_p^{\Phi} J_f^c \end{vmatrix} = 0 \tag{32}$$

where $\left|J\right|$ denotes the determinant of matrix J. Referring to Theorem A2, we have

$$\begin{aligned} &\left\| \left[\lambda - (1-\eta)\right] I \left\{ \left[\lambda - (1-\alpha)\right] I - \alpha\eta J_p^{\Phi} J_f^c \right\} - \left[-\alpha(1-\eta) J_p^{\Phi} \right] \left[-\eta J_f^c \right] \right| \\ &= \left| \left[\lambda - (1-\eta)\right] \left[\lambda - (1-\alpha)\right] I - \alpha\eta\lambda J_p^{\Phi} J_f^c \right| \\ &= 0 \end{aligned}$$

Then each μ_i (i.e., each eigenvalue of $J_p^{\Phi} J_f^c$, as defined in Lemma 1) corresponds to two eigenvalues of J_1 via the following relationship:

$$\left[\lambda - (1-\eta)\right] \left[\lambda - (1-\alpha)\right] - \alpha\eta\mu_i\lambda = 0 \tag{33}$$

i.e., the two roots of Eq. (33), denoted by $\lambda_{\pm}(\mu_i)$, are two eigenvalues of J_1. Then

$$\lambda_{\pm}(\mu_i) = \frac{(1-\eta) + (1-\alpha) + \alpha\eta\mu_i \pm \sqrt{\Delta(\mu_i)}}{2}$$

where

$$\Delta(\mu_i) = \left[(1-\eta) + (1-\alpha) + \alpha\eta\mu_i \right]^2 - 4(1-\eta)(1-\alpha)$$

Considering the value of $\Delta(\mu_i)$:

(a) If $\Delta(\mu_i) < 0$, i.e.

$$\frac{-2\sqrt{(1-\eta)(1-\alpha)} - \left[(1-\eta) + (1-\alpha)\right]}{\alpha\eta} < \mu_i < \frac{2\sqrt{(1-\eta)(1-\alpha)} - \left[(1-\eta) + (1-\alpha)\right]}{\alpha\eta} \tag{34}$$

then $\lambda_{\pm}(\mu_i)$ are complex. According to Vieta's formula, $\left|\lambda_{\pm}(\mu_i)\right| = \sqrt{\lambda_{+}(\mu_i)\lambda_{-}(\mu_i)} = \sqrt{(1-\eta)(1-\alpha)} < 1$.

(b) If $\Delta(\mu_i) \geq 0$, i.e.

$$\mu_i \le \frac{-2\sqrt{(1-\eta)(1-\alpha)}-\left[(1-\eta)+(1-\alpha)\right]}{\alpha\eta} \tag{35}$$

or

$$\mu_i \ge \frac{2\sqrt{(1-\eta)(1-\alpha)}-\left[(1-\eta)+(1-\alpha)\right]}{\alpha\eta} \tag{36}$$

then $\lambda_{\pm}(\mu_i)$ are real. Hence $|\lambda_{\pm}(\mu_i)|<1$ requires $\lambda_{+}(\mu_i)<1$ and $\lambda_{-}(\mu_i)>-1$ holding simultaneously, where $\lambda_{+}(\mu_i)<1$ is equivalent to

$$\mu_i < \frac{(1-\eta)(1-\alpha)+1-\left[(1-\eta)+(1-\alpha)\right]}{\alpha\eta}=1 \tag{37}$$

which always holds as $\mu_i \le 0$, and $\lambda_{-}(\mu_i)>-1$ is equivalent to

$$\mu_i > \frac{-1-(1-\eta)(1-\alpha)-\left[(1-\eta)+(1-\alpha)\right]}{\alpha\eta}=-\frac{(2-\alpha)(2-\eta)}{\alpha\eta} \tag{38}$$

When $0<\alpha\le 1$ and $0<\eta\le 1$, the right hand side of the equality in Eq. (38) is strictly smaller than the right hand side of Eq. (35) due to

$$-1-(1-\eta)(1-\alpha)<-2\sqrt{(1-\eta)(1-\alpha)} \tag{39}$$

Meanwhile, when Eq. (36) holds, Eq. (38) will automatically hold. Therefore, combining conditions (34)-(38), we have: for Eq. (33), $|\lambda_{\pm}(\mu_i)|<1$ if and only if condition (38) holds. Referring to Theorem A1, the proof is completed.

Remark 4. For the case in Remark 2, when $0<\alpha\le 1$ and $\eta>1$, one can still rely on Theorem 1 to check the stability. The proof is almost the same as the proof above – just note that, when $0<\alpha\le 1$ and $\eta>1$, we will always have $\Delta(\mu_i)\ge 0$, then the condition $|\lambda_{\pm}(\mu_i)|<1$ requires Eqs. (37) and (38) holding simultaneously, which yields Theorem 1.

Appendix C. Proof of Theorem 2

If $\theta = 1$, then the case degenerates to Theorem 1, and thus the equilibrium point is asymptotically stable when

$$\mu_{\min} > -\frac{(2-\alpha)(2-\theta)(2-\eta)}{\alpha\theta\eta} \tag{40}$$

If $\theta \neq 1$, the Jacobian of the dynamical system (9)+(1)+(2) evaluated at its equilibrium reads

$$J_2 = \begin{pmatrix} (1-\theta)I & 0 & \theta J_f^c \\ \eta(1-\theta)I & (1-\eta)I & \eta\theta J_f^c \\ \alpha J_p^\Phi \eta(1-\theta) & \alpha J_p^\Phi (1-\eta) & \alpha J_p^\Phi \eta\theta J_f^c + (1-\alpha)I \end{pmatrix} \tag{41}$$

whose eigenvalues λ are the solutions of

$$|\lambda I - J_2| = \begin{vmatrix} [\lambda-(1-\theta)]I & 0 & -\theta J_f^c \\ -\eta(1-\theta)I & [\lambda-(1-\eta)]I & -\eta\theta J_f^c \\ -\alpha J_p^\Phi \eta(1-\theta) & -\alpha J_p^\Phi (1-\eta) & [\lambda-(1-\alpha)]I - \alpha J_p^\Phi \eta\theta J_f^c \end{vmatrix} = 0 \tag{42}$$

In Eq. (42), swapping the first two rows of blocks and, as $-\eta(1-\theta)I$ is invertible, using Theorem A3 leads to

$$\begin{vmatrix} \frac{1}{\eta(1-\theta)}[\lambda-(1-\theta)][\lambda-(1-\eta)]I & -\frac{\theta}{1-\theta}\lambda J_f^c \\ -\alpha\lambda J_p^\Phi & [\lambda-(1-\alpha)]I \end{vmatrix} = 0$$

which, after using Theorem A2, yields

$$\left|[\lambda-(1-\theta)][\lambda-(1-\eta)][\lambda-(1-\alpha)]I - \alpha\theta\eta\lambda^2 J_p^\Phi J_f^c\right| = 0 \tag{43}$$

Therefore, the eigenvalues of J_2 are equivalent to the roots of the following equations,

$$\varphi_i(\lambda) := y(\lambda) - z_i(\lambda) = 0, \quad i = 1, 2, \cdots, N \tag{44}$$

where

$$y(\lambda) = [\lambda-(1-\alpha)][\lambda-(1-\theta)][\lambda-(1-\eta)]$$

and

$$z_i(\lambda) = \alpha\theta\eta\mu_i\lambda^2$$

The stability of the dynamical system requires the moduli of all eigenvalues of J_2, i.e., the moduli of all roots of Eq. (44), to be less than 1 (Theorem A1).

When $\alpha = 1$, Eq. (44) leads to

$$\lambda = 0 \quad \text{or} \quad \left[\lambda - (1-\theta)\right]\left[\lambda - (1-\eta)\right] - \theta\eta\mu_i\lambda = 0$$

Referring to Eq. (33), the fixed point is stable when Eq. (40) holds. The situation is the same when $\eta = 1$. This means Eq. (40) is the stability condition when $\max\{\alpha, \theta, \eta\} = 1$. Therefore, hereafter, we consider the case when $\max\{\alpha, \theta, \eta\} < 1$.

As $\max\{\alpha, \theta, \eta\} < 1$, denote

$$\rho = \min\{1-\alpha, 1-\theta, 1-\eta\} > 0$$

Then $y(0) < 0$, $y(\rho) = 0$, $z_i(0) = 0$, $z_i(\rho) \le 0$. Hence we have

$$\varphi_i(0) < 0 \quad \text{and} \quad \varphi_i(\rho) \ge 0 \quad \text{with the equality holding if and only if} \quad \mu_i = 0 \tag{45}$$

Further from Eq. (44), $\varphi_i'(\lambda) = y'(\lambda) - z_i'(\lambda)$, where

$$y'(\lambda) = \left[\lambda - (1-\alpha)\right]\left[\lambda - (1-\theta)\right] + \left[\lambda - (1-\alpha)\right]\left[\lambda - (1-\eta)\right] + \left[\lambda - (1-\theta)\right]\left[\lambda - (1-\eta)\right]$$

and

$$z_i'(\lambda) = 2\alpha\theta\eta\mu_i\lambda$$

Then

$$y'(\lambda)\begin{cases} > 0, & 0 \le \lambda < \rho \\ \ge 0, & \lambda = \rho \end{cases}, \quad z_i'(\lambda)\begin{cases} = 0, & \lambda = 0 \\ \le 0, & 0 < \lambda \le \rho \end{cases}$$

and thus

$$\varphi_i'(\lambda)\begin{cases} > 0, & 0 \le \lambda < \rho \\ \ge 0, & \lambda = \rho \end{cases} \tag{46}$$

where $\varphi_i'(\rho) = 0$ if and only if $\mu_i = 0$ and at least two of $1-\alpha$, $1-\theta$ and $1-\eta$ equal ρ. Conditions (45) and (46) then tell that, within $(0, \rho]$, $\varphi_i(\lambda) = 0$ has one and only one (single or multiple) real root, which is denoted by λ_i^{r+}, where $\lambda_i^{r+} = \rho$ if and only if $\mu_i = 0$.

The two roots of $\varphi_i'(\lambda)=0$ are

$$\tilde{\lambda}_{1,2}(\mu_i)=\frac{\left[(1-\alpha)+(1-\theta)+(1-\eta)+\alpha\theta\eta\mu_i\right]\pm\sqrt{\tilde{\Delta}(\mu_i)}}{3} \tag{47}$$

where $\tilde{\Delta}(\mu_i)$ is a quarter of the discriminant of $\varphi_i'(\lambda)$ and given in Eq. (14). By looking into the values of $\tilde{\Delta}(\mu_i)$ and $\tilde{\lambda}_{1,2}(\mu_i)$, we have the following cases:

(i) If $\tilde{\Delta}(\mu_i)\le 0$, i.e., $\mu_-\le\mu_i\le\mu_+$, where μ_- and μ_+ are the two roots of $\tilde{\Delta}(\mu_i)=0$ and given in Eqs. (15) and (16), then $\varphi_i(\lambda)$ is increasing in $(-\infty,+\infty)$ and thus has a triple root which is $\lambda_i^{r+}\in(0,\rho]$ and satisfies $|\lambda_i^{r+}|<1$.

(ii) If $\tilde{\Delta}(\mu_i)>0$ (i.e., $\mu_i<\mu_-$ or $\mu_i>\mu_+$), then $\varphi_i(\lambda)$ has two local optima achieved at $\lambda=\tilde{\lambda}_{1,2}(\mu_i)$. Based on the fact that $\varphi_i(0)<0$ and $\varphi_i'(0)>0$, we plot all possible shapes of $\varphi(\lambda)$ in Figure 8, where Figure 8(a) is impossible as according to condition (46), $\varphi_i(\lambda)$ must be strictly increasing in $(0,\lambda_i^{r+})$. Then we have the following cases (a) and (b).

(a) If $\Delta_0(\mu_i)<0$ (where $\Delta_0(\mu_i)$ is the discriminant of $\varphi_i(\lambda)$ and given in Eq. (13)), then $\varphi_i(\lambda)$ has two non-real conjugate complex roots, denoted by λ_i^{c+} and λ_i^{c-}, respectively. The possible scenarios are shown in Figure 8(e)(f). According to Vieta's formula, $\lambda_i^{r+}\lambda_i^{c+}\lambda_i^{c-}=(1-\alpha)(1-\theta)(1-\eta)$, meaning

$$|\lambda_i^{c+}|^2=|\lambda_i^{c-}|^2=\lambda_i^{c+}\lambda_i^{c-}=\frac{(1-\alpha)(1-\theta)(1-\eta)}{\lambda_i^{r+}}$$

hence $|\lambda_i^{c\pm}|^2<1$ is equivalent to

$$\lambda_i^{r+}>(1-\alpha)(1-\theta)(1-\eta) \tag{48}$$

As $\varphi_i(\lambda)$ is strictly increasing in $\lambda\in(0,\rho)$, Eq. (48) is equivalent to $\varphi_i\left((1-\alpha)(1-\theta)(1-\eta)\right)<\varphi_i(\lambda_i^{r+})=0$, i.e.

$$\mu_i > \frac{\left[(1-\alpha)(1-\theta)-1\right]\left[(1-\theta)(1-\eta)-1\right]\left[(1-\eta)(1-\alpha)-1\right]}{\alpha\theta\eta(1-\alpha)(1-\theta)(1-\eta)} \tag{49}$$

(b) If $\Delta_0(\mu_i) \geq 0$, then $\varphi_i(\lambda)$ has three real roots, and the possible scenarios are:

a) In Figure 8(b)(c)(d), $\tilde{\lambda}_{1,2}(\mu_i) > 0$, all the roots are real and nonnegative. Meanwhile, when $\lambda \geq 1$, $y(\lambda) \geq \alpha\theta\eta > 0$ and $z_i(\lambda) \leq 0$, and thus $\varphi_i(\lambda) > 0$. It means the roots of $\varphi_i(\lambda) = 0$ must all locate in $(0,1)$, hence their moduli are all less than 1.

b) In Figure 8(g)(h), $\tilde{\lambda}_{1,2}(\mu_i) < 0$, $\varphi_i(\lambda)$ has two negative real roots. Then the moduli of both negative roots are less than 1 if and only if $\tilde{\lambda}_{1,2}(\mu_i) > -1$ and $\varphi_i(-1) < 0$.

Combining a) & b) yields, if $\Delta_0(\mu_i) \geq 0$, then the moduli of all the roots of $\varphi_i(\lambda)$ are less than 1 if and only if

$$\begin{aligned}\mu_i \in & \left\{\mu_i : \tilde{\lambda}_{1,2}(\mu_i) > 0\right\} \cup \left(\left\{\mu_i : -1 < \tilde{\lambda}_{1,2}(\mu_i) < 0\right\} \cap \left\{\mu_i : \varphi_i(-1) < 0\right\}\right) \\ = & \left(\left\{\mu_i : \tilde{\lambda}_{1,2}(\mu_i) > 0\right\} \cup \left\{\mu_i : -1 < \tilde{\lambda}_{1,2}(\mu_i) < 0\right\}\right) \\ & \cap \left(\left\{\mu_i : \tilde{\lambda}_{1,2}(\mu_i) > 0\right\} \cup \left\{\mu_i : \varphi_i(-1) < 0\right\}\right)\end{aligned} \tag{50}$$

According to Eqs. (47) and (14), $\tilde{\lambda}_{1,2}(\mu_i) = 0$ requires $(1-\alpha)(1-\theta)+(1-\theta)(1-\eta)+(1-\eta)(1-\alpha) = 0$, which violates $\max\{\alpha,\theta,\eta\} < 1$; therefore, we must have $\tilde{\lambda}_{1,2}(\mu_i) \neq 0$ and thus

$$\left\{\mu_i : \tilde{\lambda}_{1,2}(\mu_i) > 0\right\} \cup \left\{\mu_i : -1 < \tilde{\lambda}_{1,2}(\mu_i) < 0\right\} = \left\{\mu_i : \tilde{\lambda}_{1,2}(\mu_i) > -1\right\} \tag{51}$$

Meanwhile, from Figure 8(b)(c)(d)(e), we can easily see that, when $\tilde{\lambda}_{1,2}(\mu_i) > 0$, one must have $\varphi_i(-1) < 0$; therefore,

$$\left\{\mu_i : \tilde{\lambda}_{1,2}(\mu_i) > 0\right\} \subset \left\{\mu_i : \varphi_i(-1) < 0\right\} \tag{52}$$

Substituting Eqs. (51) and (52) into Eq. (50) yields

$$\mu_i \in \left\{\mu_i : \tilde{\lambda}_{1,2}\left(\mu_i\right) > -1\right\} \cap \left\{\mu_i : \varphi_i\left(-1\right) < 0\right\}$$

where $\tilde{\lambda}_{1,2}\left(\mu_i\right) > -1$ is equivalent to

$$\mu_i > -\frac{\left[(1-\alpha)(1-\theta)+(1-\theta)(1-\eta)+(1-\eta)(1-\alpha)\right]+3+2\left[(1-\alpha)+(1-\theta)+(1-\eta)\right]}{2\alpha\theta\eta} \quad (53)$$

and $\varphi_i\left(-1\right) < 0$ is equivalent to

$$\mu_i > -\frac{\left[1+(1-\alpha)\right]\left[1+(1-\theta)\right]\left[1+(1-\eta)\right]}{\alpha\theta\eta} \quad (54)$$

Summarizing all the conditions above completes the proof.

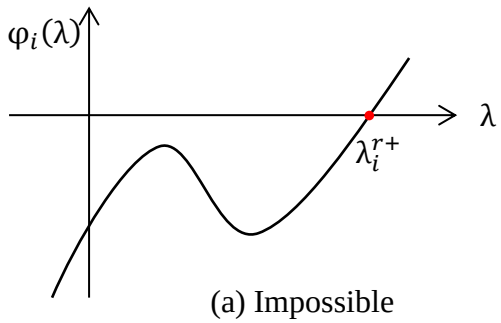

(a) Impossible

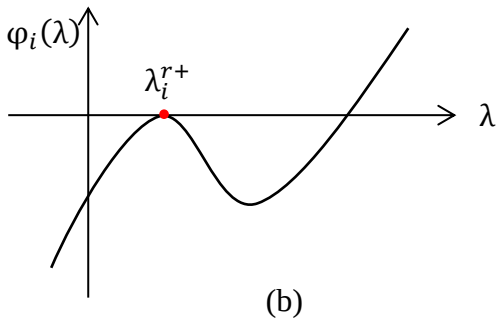

(b)

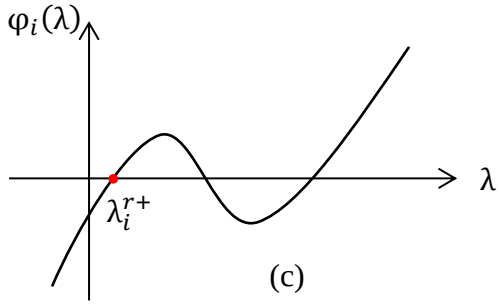

(c)

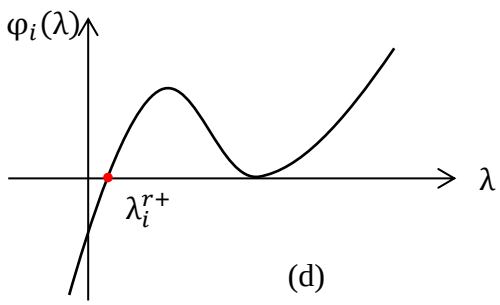

(d)

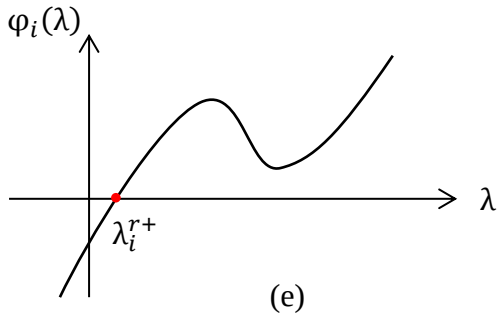

(e)

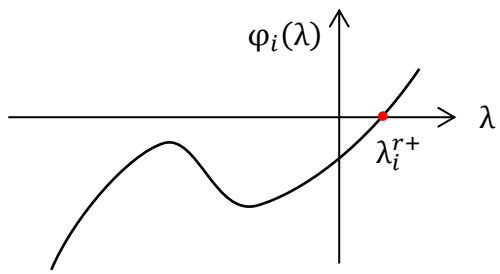

(f)

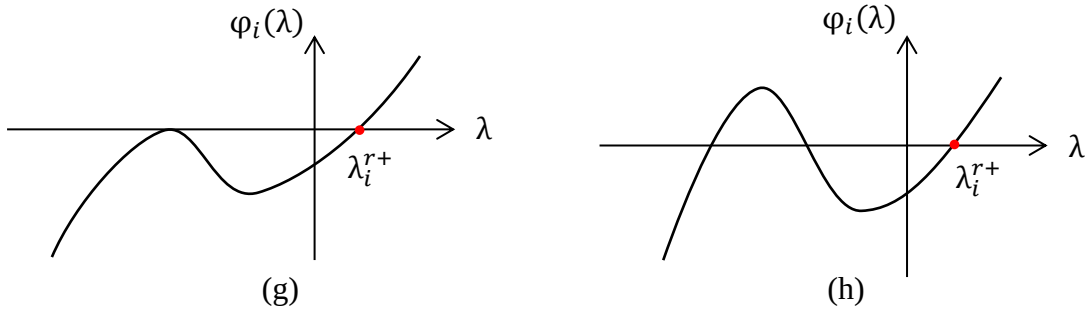

Figure 8. The possible curves of $\varphi_i(\lambda)$ when $\max\{\alpha,\theta,\eta\}<1$ and $\tilde{\Delta}(\mu_i)>0$.

Appendix D. Proof of Remark 3

When $\max\{\alpha,\theta,\eta\}\to 1$, without loss of generality, assume $\theta\to 1$. Then Eqs. (10)-(14) read $a_i=-\left[(1-\alpha)+(1-\eta)+\alpha\eta\mu_i\right]$, $h=(1-\eta)(1-\alpha)$, $g=0$, $\Delta_0(\mu_i)=h^2\left(a_i^2-4h\right)$ and $\tilde{\Delta}(\mu_i)=a_i^2-3h$. Eq. (18) always holds as it reads

$$\mu_i>\lim_{\theta\to 1^-}\frac{\left[(1-\alpha)(1-\theta)-1\right]\left[(1-\theta)(1-\eta)-1\right]\left[(1-\eta)(1-\alpha)-1\right]}{\alpha\theta\eta(1-\alpha)(1-\theta)(1-\eta)}=-\infty$$

and Eq. (19) reads

$$\mu_i>\max\left\{-\frac{(1-\alpha)(1-\eta)+3+2\left[(1-\alpha)+(1-\eta)\right]}{2\alpha\eta},-\frac{(2-\alpha)(2-\eta)}{\alpha\eta}\right\}=-\frac{(2-\alpha)(2-\eta)}{\alpha\eta}$$

Subsequently we discuss the case when $h=0$ and $h>0$, respectively.

If $h=0$, then $\Delta_0(\mu_i)=0$, and $\tilde{\Delta}(\mu_i)=a_i^2$. Then in Theorem 2,

- Condition (i) reduces to $a_i=0$, condition (ii) is invalid, and condition (iii) reduces to $a_i\neq 0$ and $\mu_i>-\frac{(2-\alpha)(2-\eta)}{\alpha\eta}$. Combining conditions (i)-(iii) yields Eq. (17).

- Condition (iv) is invalid, and condition (v) reads $a_i\neq 0$ & $\mu_i<-\frac{(2-\alpha)(2-\eta)}{\alpha\eta}$. As

when $\mu_i < -\frac{(2-\alpha)(2-\eta)}{\alpha\eta}$, we have $a_i > 1+(1-\alpha)(1-\eta) > 0$, then condition (v) is equivalent to the reverse of Eq. (17).

If $h > 0$, then

- Condition (i) reduces to $a_i^2 \le 3h$, condition (ii) to $3h < a_i^2 < 4h$, and condition (iii) to $a_i^2 \ge 4h$ & $\mu_i > -\frac{(2-\alpha)(2-\eta)}{\alpha\eta}$. Then as the union of conditions (i) and (ii) is $a_i^2 < 4h$, the union of conditions (i)-(iii) is

$$a_i^2 < 4h \quad \text{or} \quad (a_i^2 \ge 4h \ \& \ \mu_i > -\frac{(2-\alpha)(2-\eta)}{\alpha\eta})$$

$$\Leftrightarrow \ (a_i^2 < 4h \ \text{or} \ a_i^2 \ge 4h) \ \& \ (a_i^2 < 4h \ \text{or} \ \mu_i > -\frac{(2-\alpha)(2-\eta)}{\alpha\eta})$$

$$\Leftrightarrow \ a_i^2 < 4h \ \text{or} \ \mu_i > -\frac{(2-\alpha)(2-\eta)}{\alpha\eta} \tag{55}$$

where $a_i^2 < 4h$ is equivalent to

$$\frac{-2\sqrt{(1-\eta)(1-\alpha)} - [(1-\alpha)+(1-\eta)]}{\alpha\eta} < \mu_i < \frac{2\sqrt{(1-\eta)(1-\alpha)} - [(1-\alpha)+(1-\eta)]}{\alpha\eta} \tag{56}$$

whose left hand side is not less than $-\frac{(2-\alpha)(2-\eta)}{\alpha\eta}$. This means condition (55) further reduces to $\mu_i > -\frac{(2-\alpha)(2-\eta)}{\alpha\eta}$, which is Eq. (17).

- Condition (iv) is invalid, and condition (v) reduces to $a_i^2 \ge 4h$ and $\mu_i < -\frac{(2-\alpha)(2-\eta)}{\alpha\eta}$; according to Eq. (56), one can easily see that condition (v) is equivalent to the reverse of Eq. (17).

Combining the results for $h = 0$ and $h > 0$ completes the proof.

Appendix E. Proof of Theorem 3

The Jacobian matrix at the equilibrium point is calculated as

$$J_3 = \begin{pmatrix} -\hat{\eta} I & \hat{\eta} J_f^c \\ \hat{\alpha} J_p^{\Phi} & -\hat{\alpha} I \end{pmatrix} \tag{57}$$

whose eigenvalues, denoted by λ, are the roots of the following equation:

$$\left|\lambda I - J_3\right| = \begin{vmatrix} (\lambda + \hat{\eta}) I & -\hat{\eta} J_f^c \\ -\hat{\alpha} J_p^{\Phi} & (\lambda + \hat{\alpha}) I \end{vmatrix} = \left|(\lambda + \hat{\alpha})(\lambda + \hat{\eta}) I - \hat{\alpha}\hat{\eta} J_p^{\Phi} J_f^c\right| = 0$$

where the second equality holds due to Theorem A2. Then each eigenvalue μ_i of $J_p^{\Phi} J_f^c$ corresponds to two eigenvalues of J_3 via the following relationship:

$$(\lambda + \hat{\alpha})(\lambda + \hat{\eta}) - \hat{\alpha}\hat{\eta}\mu_i = 0, \quad i = 1, 2, \cdots, N \tag{58}$$

whose roots are

$$\frac{-(\hat{\alpha} + \hat{\eta}) \pm \sqrt{(\hat{\alpha} + \hat{\eta})^2 - 4\hat{\alpha}\hat{\eta}(1 - \mu_i)}}{2} \tag{59}$$

If the two roots in Eq. (59) are real, then they are negative as $\mu_i \le 0$; if they are complex, then their real parts are negative. Referring to Theorem A1, the equilibrium points of system (22)-(23) are always locally asymptotically stable. This completes the proof.

Appendix F. Proof of Theorem 4

The Jacobian at the equilibrium point is calculated as

$$J_4 = \begin{pmatrix} -\hat{\theta} I & 0 & \hat{\theta} J_f^c \\ \hat{\eta} I & -\hat{\eta} I & 0 \\ 0 & \hat{\alpha} J_p^{\Phi} & -\hat{\alpha} I \end{pmatrix}$$

whose eigenvalues, denoted by λ, are given by the solutions of the following equation,

$$\left|\lambda I - J_4\right| = \begin{vmatrix} (\lambda + \hat{\theta}) I & 0 & -\hat{\theta} J_f^c \\ -\hat{\eta} I & (\lambda + \hat{\eta}) I & 0 \\ 0 & -\hat{\alpha} J_p^{\Phi} & (\lambda + \hat{\alpha}) I \end{vmatrix} = 0 \tag{60}$$

Swapping the top two rows of blocks and referring to Theorem A3, Eq. (60) leads to

$$
\begin{aligned}
&\left|-\hat{\eta}I\right|\left|\begin{pmatrix} 0 & -\hat{\theta}J_f^c \\ -\hat{\alpha}J_p^{\Phi} & (\lambda+\hat{\alpha})I \end{pmatrix}-\begin{pmatrix} (\lambda+\hat{\theta})I \\ 0 \end{pmatrix}\left(-\frac{1}{\hat{\eta}}I\right)\begin{pmatrix}(\lambda+\hat{\eta})I & 0\end{pmatrix}\right| \\
&=\left|-\hat{\eta}I\right|\begin{vmatrix} \frac{1}{\hat{\eta}}(\lambda+\hat{\theta})(\lambda+\hat{\eta})I & -\hat{\theta}J_f^c \\ -\hat{\alpha}J_p^{\Phi} & (\lambda+\hat{\alpha})I \end{vmatrix} \\
&=\left|-I\right|\left|(\lambda+\hat{\theta})(\lambda+\hat{\eta})(\lambda+\hat{\alpha})I-\hat{\alpha}\hat{\theta}\hat{\eta}J_p^{\Phi}J_f^c\right| \\
&=0
\end{aligned}
$$

(where the second equality holds due to Theorem A2), i.e.

$$\left|(\lambda+\hat{\theta})(\lambda+\hat{\eta})(\lambda+\hat{\alpha})I-\hat{\alpha}\hat{\theta}\hat{\eta}J_p^{\Phi}J_f^c\right|=0 \tag{61}$$

Define

$$\varphi(\lambda)=(\lambda+\hat{\theta})(\lambda+\hat{\eta})(\lambda+\hat{\alpha}) \tag{62}$$

then according to Eq. (61), each eigenvalue μ_i of $J_p^{\Phi}J_f^c$ corresponds to three eigenvalues of J_4, which are the roots of

$$\varphi(\lambda)-\hat{\alpha}\hat{\theta}\hat{\eta}\mu_i=0 \tag{63}$$

Depending on the values of $\hat{\alpha}$, $\hat{\theta}$ and $\hat{\eta}$, we have the following two cases to discuss.

(1) When $\hat{\alpha}=\hat{\theta}=\hat{\eta}$, Eq. (63) has three identical roots equal to $\hat{\alpha}\mu_i^{1/3}-\hat{\alpha}$, which are real and negative as $\mu_i\le 0$. This proves part (i) in Theorem 4.

(2) When $\hat{\alpha}$, $\hat{\theta}$ and $\hat{\eta}$ are not all equal, according to Vieta's formula, the product of the three roots is $\hat{\alpha}\hat{\theta}\hat{\eta}(\mu_i-1)<0$, meaning Eq. (63) has at least one root which is real and negative; depending on the value of μ_i, the other two roots are either both real or both complex and conjugate. To find out under what circumstance the complex roots would appear, by letting $\varphi'(\lambda)=0$, we know the local minimum of $\varphi(\lambda)$ (Figure 9) is achieved at

$$\lambda^*=\frac{-(\hat{\alpha}+\hat{\theta}+\hat{\eta})+\sqrt{(\hat{\alpha}+\hat{\theta}+\hat{\eta})^2-3(\hat{\alpha}\hat{\theta}+\hat{\theta}\hat{\eta}+\hat{\eta}\hat{\alpha})}}{3}$$

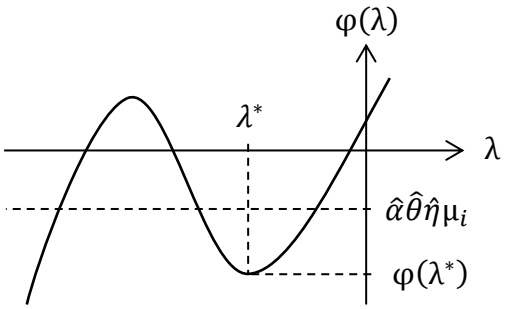

Figure 9. The curve of $\varphi(\lambda)$.

Obviously, according to Figure 9, Eq. (63) will have complex roots if and only if $\hat{\alpha}\hat{\theta}\hat{\eta}\mu_i < \varphi(\lambda^*)$. Then we have the following two subcases.

(2a) When $\hat{\alpha}\hat{\theta}\hat{\eta}\mu_i \geq \varphi(\lambda^*)$, all the three roots of Eq. (63) are real and negative.

(2b) When $\hat{\alpha}\hat{\theta}\hat{\eta}\mu_i < \varphi(\lambda^*)$, $\varphi(\lambda)$ will have two non-real complex roots. To know in what circumstance the complex roots will have negative real parts, we rewrite Eq. (63) as

$$\varphi(\lambda) - \hat{\alpha}\hat{\theta}\hat{\eta}\mu_i = (\lambda + b)(\lambda^2 - 2k\lambda + q) = 0, \quad k^2 - q < 0 \tag{64}$$

i.e., the real root is $-b$ and the complex roots are $k \pm \mathrm{i}\sqrt{q - k^2}$. Substituting Eq. (62) into Eq. (64) reads

$$\begin{aligned}&\lambda^3 + (\hat{\alpha} + \hat{\theta} + \hat{\eta})\lambda^2 + (\hat{\alpha}\hat{\theta} + \hat{\theta}\hat{\eta} + \hat{\eta}\hat{\alpha})\lambda + \hat{\alpha}\hat{\theta}\hat{\eta} - \hat{\alpha}\hat{\theta}\hat{\eta}\mu_i \\ &= \lambda^3 + (b - 2k)\lambda^2 + (q - 2bk)\lambda + bq\end{aligned}$$

meaning

$$\hat{\alpha} + \hat{\theta} + \hat{\eta} = b - 2k \tag{65}$$

$$\hat{\alpha}\hat{\theta} + \hat{\theta}\hat{\eta} + \hat{\eta}\hat{\alpha} = q - 2bk \tag{66}$$

$$\hat{\alpha}\hat{\theta}\hat{\eta} - \hat{\alpha}\hat{\theta}\hat{\eta}\mu_i = bq \tag{67}$$

Solving μ_i from Eqs. (65)-(67) gives

$$\mu_i = \mu^* - \frac{2k\left[(\hat{\alpha}\hat{\theta} + \hat{\theta}\hat{\eta} + \hat{\eta}\hat{\alpha}) + (\hat{\alpha} + \hat{\theta} + \hat{\eta} + 2k)^2\right]}{\hat{\alpha}\hat{\theta}\hat{\eta}} \tag{68}$$

where μ^* is defined as

$$\mu^* \triangleq \frac{\hat{\alpha}\hat{\theta}\hat{\eta} - \left(\hat{\alpha}+\hat{\theta}+\hat{\eta}\right)\left(\hat{\alpha}\hat{\theta}+\hat{\theta}\hat{\eta}+\hat{\eta}\hat{\alpha}\right)}{\hat{\alpha}\hat{\theta}\hat{\eta}}$$

From Eq. (68), we have $\mu_i > \mu^*$ ($\mu_i < \mu^*$) if and only if $k < 0$ ($k > 0$), where k is the real part of the non-real complex roots as mentioned earlier. Since Eq. (63) will have non-real complex roots when and only when $\hat{\alpha}\hat{\theta}\hat{\eta}\mu_i < \varphi\left(\lambda^*\right)$ (as mentioned in the very beginning of this subcase), then it will have complex roots with negative real parts ($k < 0$) when $\mu_i > \mu^*$ and $\hat{\alpha}\hat{\theta}\hat{\eta}\mu_i < \varphi\left(\lambda^*\right)$, i.e., $\hat{\alpha}\hat{\theta}\hat{\eta}\mu_i \in \left(\hat{\alpha}\hat{\theta}\hat{\eta}\mu^*, \varphi\left(\lambda^*\right)\right)$, and complex roots with positive real parts when $\mu_i < \mu^*$. Note that $\hat{\alpha}\hat{\theta}\hat{\eta}\mu^* < \varphi\left(\lambda^*\right)$ holds because

$$\begin{aligned}
&\varphi\left(\lambda^*\right) - \hat{\alpha}\hat{\theta}\hat{\eta}\mu^* \\
&= \frac{2}{27}\left[\left(\hat{\alpha}+\hat{\theta}+\hat{\eta}\right)^2 - 3\left(\hat{\alpha}\hat{\theta}+\hat{\theta}\hat{\eta}+\hat{\eta}\hat{\alpha}\right)\right]\left[\left(\hat{\alpha}+\hat{\theta}+\hat{\eta}\right) - \sqrt{\left(\hat{\alpha}+\hat{\theta}+\hat{\eta}\right)^2 - 3\left(\hat{\alpha}\hat{\theta}+\hat{\theta}\hat{\eta}+\hat{\eta}\hat{\alpha}\right)}\right] \\
&\quad + \frac{8}{9}\left(\hat{\alpha}+\hat{\theta}+\hat{\eta}\right)\left(\hat{\alpha}\hat{\theta}+\hat{\theta}\hat{\eta}+\hat{\eta}\hat{\alpha}\right) \\
&> 0
\end{aligned}$$

where the term in the square root is nonnegative due to

$$\left(\hat{\alpha}+\hat{\theta}+\hat{\eta}\right)^2 - 3\left(\hat{\alpha}\hat{\theta}+\hat{\theta}\hat{\eta}+\hat{\eta}\hat{\alpha}\right) = \frac{1}{2}\left[\left(\hat{\alpha}-\hat{\theta}\right)^2 + \left(\hat{\theta}-\hat{\eta}\right)^2 + \left(\hat{\eta}-\hat{\alpha}\right)^2\right]$$

Combining subcase (2b) with (2a), the equilibrium point is stable when $\mu_i > \mu^*$, and unstable when $\mu_i < \mu^*$, which proves part (ii) in Theorem 4. The whole theorem is thus proved.

References

Bie, J., Lo, H.K., 2010. Stability and attraction domains of traffic equilibria in a day-to-day dynamical system formulation. Transportation Research Part B 44 (1), 90-107.

Bifulco, G.N., Cantarella, G.E., Simonelli, F., Velonà, P., 2016. Advanced traveller information systems under recurrent traffic conditions: Network equilibrium and stability.

Transportation Research Part B 92, 73-87.

Cantarella, G.E., Cascetta, E., 1994. Deterministic and stochastic process models for traffic assignment. Quaderno del Dipartimento di Ingegneria dei Trasporti dell'Universita' degli Studi di Napoli Federico II, Italy.

Cantarella, G.E., Cascetta, E., 1995. Dynamic processes and equilibrium in transportation networks: Towards a unifying theory. Transportation Science 29 (4), 305-329.

Cascetta, E., 1989. A stochastic process approach to the analysis of temporal dynamics in transportation networks. Transportation Research Part B 23 (1), 1-17.

Cascetta, E., Cantarella, G.E., 1991. A day-to-day and within-day dynamic stochastic assignment model. Transportation Research Part A 25 (5), 277-291.

Cascetta, E., Cantarella, G.E., 1993. Modelling dynamics in transportation networks: State of the art and future developments. Simulation Practice and Theory 1 (2), 65-91.

Cho, H., Hwang, M., 2005. Day-to-day vehicular flow dynamics in intelligent transportation network. Mathematical and Computer Modelling 41 (4-5), 501-522.

Delle Site, P., 2018. A mixed-behaviour equilibrium model under predictive and static Advanced Traveller Information Systems (ATIS) and state-dependent route choice. Transportation Research Part C 86, 549-562.

Emmerink, R.H., Axhausen, K.W., Nijkamp, P., Rietveld, P., 1995. Effects of information in road transport networks with recurrent congestion. Transportation 22 (1), 21-53.

Friesz, T.L., Bernstein, D., Mehta, N.J., Tobin, R.L., Ganjalizadeh, S., 1994. Day-to-day dynamic network disequilibria and idealized traveler information systems. Operations Research 42 (6), 1120-1136.

Guo, X., 2013. Toll sequence operation to realize target flow pattern under bounded rationality. Transportation Research Part B 56, 203-216.

Guo, R., Yang, H., Huang, H.J., 2013. A discrete rational adjustment process of link flows in traffic networks. Transportation Research Part C 34, 121-137.

Guo, R., Yang, H., Huang, H.J., Tan, Z.J., 2015. Link-based day-to-day network traffic dynamics and equilibria. Transportation Research Part B 71, 248-260.

Guo, R., Yang, H., Huang, H., Tan, Z., 2016. Day-to-day flow dynamics and congestion control. Transportation Science 50 (3), 982-997.

Han, L., Du, L., 2012. On a link-based day-to-day traffic assignment model. Transportation Research Part B 46 (1), 72-84.

He, X., Guo, X., Liu, H.X., 2010. A link-based day-to-day traffic assignment model. Transportation Research Part B 44 (4), 597-608.

Horn, R.A., Johnson, C.R., 2013. Matrix Analysis, 2nd ed. Cambridge University Press, New York.

Horowitz, J.L., 1984. The stability of stochastic equilibrium in a two-link transportation network. Transportation Research Part B 18 (1), 13-28.

Hu, T.Y., Mahmassani, H.S., 1997. Day-to-day evolution of network flows under real-time information and reactive signal control. Transportation Research Part C 5 (1), 51-69.

Huang, H.J., Liu, T.L., Yang, H., 2008. Modeling the evolutions of day-to-day route choice and year-to-year ATIS adoption with stochastic user equilibrium. Journal of Advanced Transportation 42 (2), 111-127.

Jha, M., Madanat, S., Peeta, S., 1998. Perception updating and day-to-day travel choice dynamics in traffic networks with information provision. Transportation Research Part C 6 (3), 189-212.

Jin, W., 2007. A dynamical system model of the traffic assignment problem. Transportation Research Part B 41 (1), 32-48.

Khalil, H.K., 2002. Nonlinear Systems, third ed. Prentice Hall, Upper Saddle River, NJ.

Lebovitz, N.R., n.d. Chapter 9: Stability II: Maps and Periodic Orbits. Ordinary Differential Equations. http://people.cs.uchicago.edu/∼lebovitz/odes.html

Li, X., Liu, W., Yang, H., 2018. Traffic dynamics in a bi-modal transportation network with information provision and adaptive transit services. Transportation Research Part C 91, 77-98.

Liu, W., Li, X., Zhang, F., Yang, H., 2017. Interactive travel choices and traffic forecast in a doubly dynamical system with user inertia and information provision. Transportation Research Part C 85, 711-731.

Mahmassani, H.S., Stephan, D.G., 1988. Experimental investigation of route and departure time choice dynamics of urban commuters. Transportation Research Record 1203, 69-84.

Mounce, R., Carey, M., 2011. Route swapping in dynamic traffic networks. Transportation Research Part B 45 (1), 102-111.

Nagurney, A., Zhang, D., 1997. Projected dynamical systems in the formulation, stability analysis, and computation of fixed-demand traffic network equilibria. Transportation Science 31 (2), 147-158.

Qi, H., Ma, S., Jia, N., Wang, G., 2019. Individual response modes to pre-trip information in congestible networks: laboratory experiment. Transportmetrica A 15 (2), 376-395.

Rapoport, A., Gisches, E.J., Daniel, T., Lindsey, R., 2014. Pre-trip information and route-choice decisions with stochastic travel conditions: Experiment. Transportation

Research Part B 68, 154-172.

Smith, M.J., 1984. The stability of a dynamic model of traffic assignment - An application of a method of lyapunov. Transportation Science 18 (3), 245-252.

Smith, M.J., Mounce, R., 2011. A splitting rate model of traffic re-routeing and traffic control. Transportation Research Part B 45, 1389-1409.

Smith, M.J., Watling, D.P., 2016. A route-swapping dynamical system and Lyapunov function for stochastic user equilibrium. Transportation Research Part B 85, 132-141.

Watling, D., 1999. Stability of the stochastic equilibrium assignment problem: A dynamical systems approach. Transportation Research Part B 33 (4), 281-312.

Watling, D.P., Cantarella, G.E., 2015. Model representation & decision-making in an ever-changing world: The role of stochastic process models of transportation systems. Networks and Spatial Economics 15 (3), 843-882.

Xiao, L., Lo, H., 2015. Combined route choice and adaptive traffic control in a day-to-day dynamical system. Networks and Spatial Economics 15 (3), 697-717.

Xiao, F., Shen, M., Xu, Z., Li, R., Yang, H., Yin, Y., 2019. Day-to-day flow dynamics for stochastic user equilibrium and a general Lyapunov function. Transportation Science 53 (3), 683-694.

Xiao, F., Yang, H., Ye, H., 2016. Physics of day-to-day network flow dynamics. Transportation Research Part B 86, 86-103.

Yang, H., Kitamura, R., Jovanis, P.P., Vaughn, K.M., Abdel-Aty, M.A., 1993. Exploration of route choice behavior with advanced traveler information using neural network concepts. Transportation 20 (2), 199-223.

Yang, F., Zhang, D., 2009. Day-to-day stationary link flow pattern. Transportation Research Part B 43 (1), 119-126.

Ye, H., Xiao, F., Yang, H., 2018. Exploration of day-to-day route choice models by a virtual experiment. Transportation Research Part C 94, 220-235.

Ye, H., Yang, H., 2013. Continuous price and flow dynamics of tradable mobility credits. Transportation Research Part B 57, 436-450.

Ye, H., Yang, H., 2017. Rational behavior adjustment process with boundedly rational user equilibrium. Transportation Science 51 (3), 968-980.

Ye, H., Yang, H., Tan, Z., 2015. Learning marginal-cost pricing via a trial-and-error procedure with day-to-day flow dynamics. Transportation Research Part B 81, 794-807.

Yu, Y., Han, K., Ochieng, W., 2020. Day-to-day dynamic traffic assignment with imperfect information, bounded rationality and information sharing. Transportation Research Part

C 114, 59-83.

Zhang, F., 2011. Matrix Theory: Basic Results and Techniques, 2nd ed. Springer, New York.

Zhang, D., Nagurney, A., Wu, J., 2001. On the equivalence between stationary link flow patterns and traffic network equilibria. Transportation Research Part B 35 (8), 731-748.